

# The oligogenic inheritance test GCOD detects risk genes and their interactions in congenital heart defects

Maureen Pittman,<sup>1,2,6</sup> Kihyun Lee,<sup>1,3,6</sup> Franco Felix,<sup>1</sup> Yu Huang,<sup>1</sup> Adrienne Lam,<sup>1</sup> Mauro W. Costa,<sup>1</sup> Deepak Srivastava,<sup>1,4</sup> and Katherine S. Pollard<sup>1,2,5</sup>

<sup>1</sup>Gladstone Institutes, San Francisco, California 94158, USA; <sup>2</sup>Department of Epidemiology and Biostatistics, University of California, San Francisco, California 94158, USA; <sup>3</sup>College of Pharmacy, Ewha Womans University, Seoul 03760, Republic of Korea;

<sup>4</sup>Department of Pediatrics, University of California, San Francisco, California 94158, USA; <sup>5</sup>Chan Zuckerberg Biohub, San Francisco, California 94158, USA

Exome sequencing of thousands of families has revealed many risk genes for congenital heart defects (CHDs), yet most cases cannot be explained by a single causal mutation. Even within the same family, individuals carrying a particular mutation in a known risk gene often demonstrate variable phenotypes, suggesting the presence of genetic modifiers. To explore oligogenic causes of CHD without assessing billions of variant combinations, we develop an efficient, simulation-based method to detect gene sets that carry co-occurring damaging variants in probands at a higher rate than expected given parental genotypes. We implement this approach in software called Gene Combinations in Oligogenic Disease (GCOD) and apply it to a cohort of 3377 CHD trios with exome sequencing. This analysis detects 160 gene pairs in which damaging variants are transmitted with higher-than-expected frequency to CHD probands but rarely or never appear in combination in their unaffected parents. Stratifying by specific phenotypes and considering gene combinations of higher orders yields an additional 6026 gene sets. Genes found in oligogenic sets are overrepresented in pathways related to heart development and often co-occur in sets of cell type marker genes from single-cell expression data. Compound heterozygosity of the newly identified digenic pair *Gata6–Por* leads to higher CHD incidence in mice compared with single hemizygotes, validating predicted genetic interactions. As genome sequencing is applied to more families and other disorders, GCOD will enable detection of increasingly large, novel gene combinations, shedding light on combinatorial causes of genetic diseases.

[Supplemental material is available for this article.]

Many diseases are genetically heterogeneous such that damaging variants at different genetic loci can lead to a common phenotype (Veenstra-Vanderweele et al. 2004; Akhirome et al. 2017). Complex genetic architecture has impeded our ability to identify causal variants and genes, despite increasingly large cohorts with exome or whole-genome sequencing. For instance, multigenerational family studies have found that some types of congenital heart defects (CHDs) have heritability estimates of 70%–90% (Cripe et al. 2004; McBride et al. 2005; Hinton et al. 2007; Pierpont et al. 2018), but just 9% of probands have a damaging variant in a monogenic CHD gene that is not shared by an unaffected family member (Sierant et al. 2025). This indicates that although most defects can be explained in large part by patient genetics, our current knowledge is insufficient to pinpoint the full genetic origin of most individual cases. In addition to environmental factors, unexplained cases presumably involve damaging variants in splice sites or regulatory regions, as well as cryptic risk genes that lack statistical evidence of association. The latter can occur owing to incomplete penetrance and variable expressivity of gene lesions, in which carriers differ in the presence and severity of disease symptoms (Janku et al. 1980; Parker and Landstrom 2021; Kingdom and Wright 2022). A potential explanation for these phenomena is oligogenic inheritance, or a type of inheritance in

which a few variants are required in combination to cause a particular phenotype (Kousi and Katsanis 2015).

Previous work has validated an instance of oligogenic inheritance in CHD (Gifford et al. 2019), as well as speculated a role for oligogenic inheritance in other developmental disorders like autism spectrum disorder (Schaaf et al. 2011; Wenger et al. 2016). Although these studies discovered specific disease-causing gene and variant combinations, they relied on known risk genes and existing functional information to propose testable hypotheses. Alternatively, one could enumerate and prioritize all damaging variant combinations in an automated and statistically rigorous manner. But this strategy is complicated by combinatorial explosion: Given that each human genome typically contains 40,000 to 200,000 variants at <0.5% minor allele frequency (MAF) (The 1000 Genomes Project Consortium 2015), an analysis of all possible rare variant pairs yields between 8 billion to nearly 20 trillion combinations per individual, necessitating a priori identification of a limited set of test loci at the variant level (Cordell 2009). Even aggregating variants in order to test pairwise gene-by-gene combinations necessitates very large sample sizes, although this can be mitigated by the use of parental controls in trio studies (Gauderman 2002).

Despite these difficulties, there are existing methods that scan the genome for possible oligogenic disease combinations. ORVAL accepts a small list of variants as input and provides gene and variant annotations to a predictor that assesses potential oligogenic

**<sup>6</sup>These authors contributed equally to this work.**

Corresponding authors: [deepak.srivastava@gladstone.ucsf.edu](mailto:deepak.srivastava@gladstone.ucsf.edu), [kpollard@gladstone.ucsf.edu](mailto:kpollard@gladstone.ucsf.edu)

Article published online before print. Article, supplemental material, and publication date are at <https://www.genome.org/cgi/doi/10.1101/gr.281141.125>. Freely available online through the *Genome Research* Open Access option.

© 2026 Pittman et al. This article, published in *Genome Research*, is available under a Creative Commons License (Attribution-NonCommercial 4.0 International), as described at <http://creativecommons.org/licenses/by-nc/4.0/>.

combinations (Renaux et al. 2019; Versbraegen et al. 2023). Similarly, the high-throughput oligogenic prioritizer (Hop) identifies potential oligogenic combinations from more extensive whole-exome sequencing (WES) variant data and incorporates phenotype ontology information (Gravel et al. 2024). However, these tools only offer oligogenic hypotheses for individuals without leveraging information from other sequenced patients. In contrast, the Digenic method aggregates rare variants at the gene level across a disease cohort and assesses the statistical significance of each gene pair based on its prevalence (Kerner et al. 2020), although this method is limited to oligogenic combinations of only two genes. RareComb is another software that tests at the cohort level, identifying gene combinations found at greater frequency in cases compared with controls (Pounraja and Girirajan 2022). Neither of these cohort methods incorporates parental sequencing data, which are especially useful in reducing false positives found as a result of population stratification (Schaid and Sommer 1994; Ewens 1999). It logically follows that the high-effect causal variants are likely transmitted separately from each unaffected parent or include at least one de novo mutation; thus, incorporating parental transmission data is potentially a powerful tool to reduce false positives, increase confidence in the phenotypic relevance of variants, and correct for population structure.

To address this gap, we developed the tool Gene Combinations in Oligogenic Disease (GCOD), an algorithmic framework that uses simulation experiments to identify disease gene sets that carry rare damaging variants significantly more often than expected given parental genotypes. In this study, we demonstrate the robustness and efficiency of GCOD, applying it to whole exomes to identify and assess sets of genes with co-occurring rare variants in CHD.

## Results

### Computational identification of pathogenic gene sets

We developed an algorithm to predict pathogenic gene sets using exome or whole-genome sequencing data and implemented it in software entitled GCOD. The method involves four main steps (Fig. 1): select variants of interest based on predicted pathogenicity or other criteria, enumerate sets of genes with co-occurring variants, count the number of proband carriers of each gene set, and evaluate the statistical significance of gene set co-occurrence counts given the parental genotypes. An optional fifth step repeats the process for healthy siblings or pseudosiblings (Yu and Deng 2011) as a control. GCOD can be viewed as an extension of the transmission disequilibrium test (TDT), in which the unit being tested is an observed co-occurrence of variants in a group of genes, rather than observed transmissions at a single genomic location (Spielman et al. 1993) or within a single gene (He et al. 2017). Details and options for each step of GCOD follow.

First, users provide a list of damaging variants meeting some criteria of interest from each individual in the data set (Fig. 1A). GCOD then enumerates all combinations of genes that contain co-occurring damaging variants in each proband (Fig. 1B), retaining only those combinations observed in multiple families (referred to as “candidate sets”). By changing the definition of damaging, different scenarios can be explored, from small gene sets with very rare co-occurring variants of high impact to larger gene sets that include small-effect, possibly damaging variants

that could modify the effects of other primary disease-causing variant(s) or otherwise contribute to a polygenic signal.

Here we use the terms “oligogenic transmission” and “oligogenic inheritance” to describe an event in which qualifying variants were inherited separately from both parents or include a de novo mutation, such that an unaffected parent did not also carry that same combination of variants. The count of observed oligogenic transmissions of the gene set to probands is the test statistic. GCOD provides two options for gene set testing, assessing either all digenic pairs observed in multiple probands (“pairs” mode) or including larger gene sets (“highest-order” mode). To reduce the number of tested hypotheses when possible, the “highest-order” algorithm first considers all digenic pairs and merges these up to the largest gene candidate set observed among a unique group of probands. For example, two probands carrying damaging variants in seven genes share 21 unique gene pairs, 35 unique gene trios, and so on (Supplemental Fig. 1). If no other probands carry co-occurring variants in two or more genes of the set, GCOD’s highest-order mode tests only the seven-gene set, while considering none of the 119 other lower-order combinations. But if a third proband carries qualifying variants in four of those seven genes, that gene quartet (with a count of three carriers) is also considered a “highest-order” candidate and is tested along with the seven-gene set (with a count of two carriers). The algorithm efficiently checks for additional transmissions of gene subsets, identifying and producing a co-occurrence count for all highest-order candidate sets.

In the third step, GCOD performs simulations based on parental genotypes under the assumption that joint variant inheritance has no relationship to disease phenotype (Fig. 1C). In each iteration, one hypothetical offspring is simulated for each parental pair as follows. We assume that damaging parental variants have a 50% chance of being passed to the simulated offspring and model different genes independently (for caveats, see Discussion). After simulating inherited variants, GCOD simulates de novo variants using previous estimates of per-gene de novo mutation probabilities (Samocho et al. 2014). Using one simulated child from each family in the cohort, we tally the number of times a given gene set was transmitted with oligogenic inheritance.

In the fourth step, the offspring simulation is repeated over many iterations to generate a null distribution of expected transmission counts, which is compared with that observed among probands. We calculate the probability of no overtransmission for each candidate gene set as the proportion of iterations with a simulated count equal to or greater than the number of probands (Fig. 1D). GCOD returns the full list of candidate sets along with the *P*-values associated with their transmission to probands. Multiple testing corrections are then applied (for details, see Methods; for caveats, see Discussion). We refer to the resulting statistically significant gene sets as “oligogenic sets.”

In an optional fifth step, GCOD repeats this entire procedure for sibling controls. If healthy siblings have been sequenced, these may be used. Otherwise, GCOD generates a genotype for a pseudosibling of each proband, a hypothetical sibling who has inherited the parental alleles that were not transmitted to the affected individual (Fig. 1E; Yu and Deng 2011). Siblings, unlike pseudosiblings, carry some variants inherited by the proband. They also can be assessed for the phenotype, whereas pseudosiblings cannot. Siblings without a diagnosis and pseudosiblings are typically presumed to be unaffected, although this is not always true; siblings must be deeply phenotyped past the typical age of onset to rule out disease, and pseudosiblings have unknown phenotypes. With these caveats in mind, it can be helpful to consider both

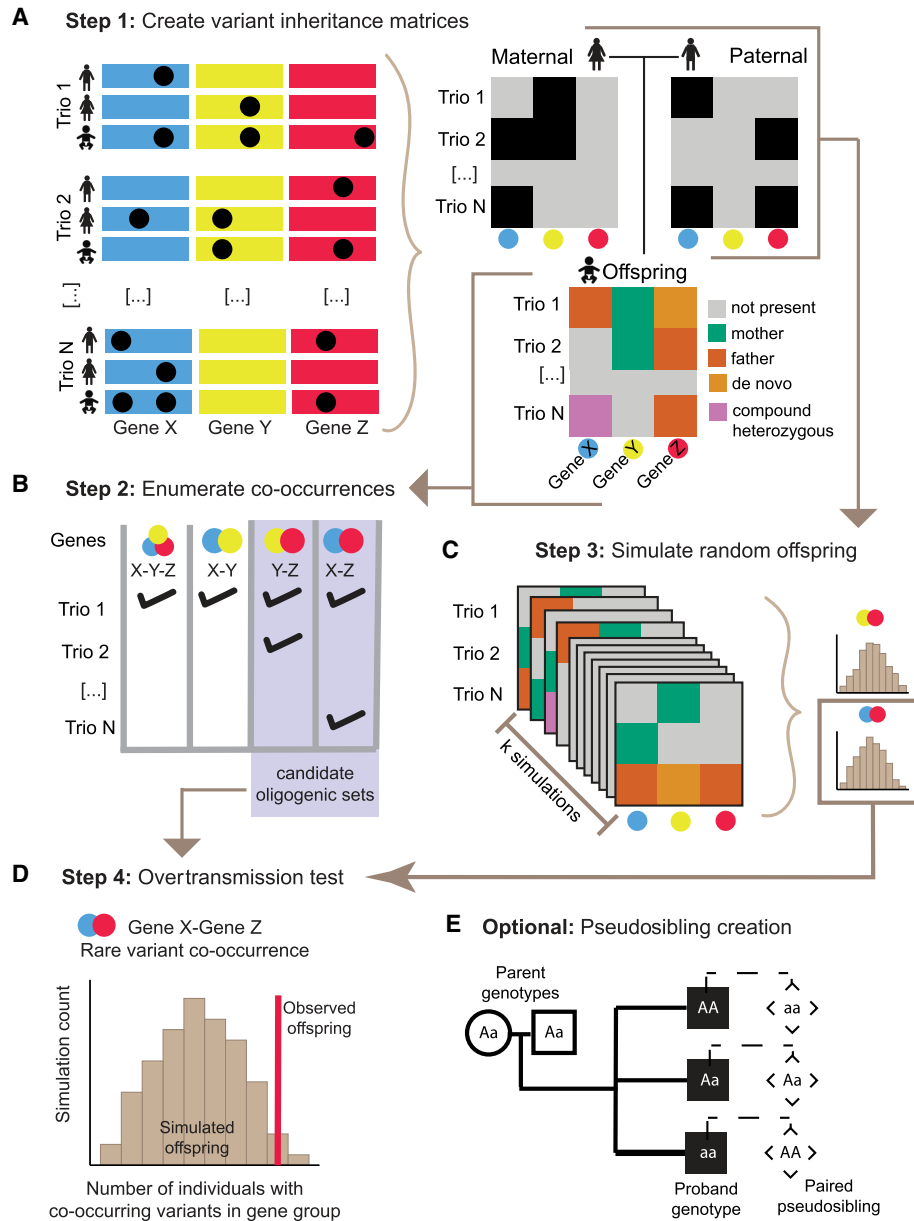


**Figure 1.** The GCOD approach identifies sets of genes that interact in oligogenic disease. (A) Step 1. Users submit a list of variants of interest or define criteria for some level of “rare” or “predicted damaging.” These variants are summarized in two binary gene-by-trio matrices that denote whether at least one damaging allele was present in each of the maternal and paternal genomes, as well as an offspring matrix that encodes damaging variant presence and provenance. The variant(s) in each gene can be only maternally derived, only paternally derived, compound heterozygous, or de novo. (B) Step 2. From the offspring matrix, GCOD enumerates the candidate sets of genes for which variants occur in multiple probands, including only combinations not transmitted from a single parent. (C) Step 3. An offspring is created from the genotypes of each pair of parents over a minimum of 10,000 simulated cohorts, yielding a distribution of simulated co-occurrence counts for each candidate set. (D) Step 4. For a given candidate set, the simulated distribution is compared to the observed number in cohort probands to compute a *P*-value. (E) Optionally, GCOD derives pseudosibling genotypes from the parental alleles not transmitted to the proband for comparative analysis.

types of controls when available. Users can exclude any significant candidate sets that also appear in (pseudo-)siblings. To assess overall evidence that a phenotype is likely oligogenic, users can explore whether probands carry more overtransmitted gene sets compared with (pseudo-)siblings.

**Comparison of resource use and type-I error rate**

We first compared GCOD to a multilocus generalization of the TDT (mTDT), which ran efficiently but yielded no significantly

overtransmitted gene sets, despite only testing pairs observed at least twice as in GCOD (Supplemental Table S1). We therefore focused on two other software tools that use variant data from multi-individual data sets to find gene combinations statistically associated with a given phenotype. Digenic is a two-locus variant aggregation test that identifies gene or variant combinations using WES data and can be run using case-only data (Kerner et al. 2020). RareComb identifies pairs and higher-order combinations of genes enriched for co-occurring variants in cases but not controls

(Pounraja and Girirajan 2022). To benchmark these three approaches, we leveraged WES of 3377 trios composed of a CHD proband and their unaffected parents, which were previously sequenced by the Pediatric Cardiac Genomics Consortium (PCGC) (Pediatric Cardiac Genomics Consortium 2013; Hoang et al. 2018; Morton et al. 2021) (obtained from the NCBI database of Genotypes and Phenotypes [dbGaP; <https://dbgap.ncbi.nlm.nih.gov/home/>] under accession number phs000571.v7.p3). To evaluate the type-I error for each method, we estimated the false-positive rate (FPR) using gene combinations based on three expected-null variant sets: rare proband synonymous variants, rare damaging proband nonsynonymous variants in which the identities of the carriers are randomly shuffled, and rare damaging pseudosibbling variants with CADD scores in the top 0.5% exome-wide. In addition to FPR, we also assessed runtime and peak memory usage for each method (Fig. 2).

We found that GCOD runs notably faster than Digenic at cohort sizes up to 1000 but takes the same amount of time on the full cohort of 3377 trios (Fig. 2A). RareComb runs the fastest at cohort

sizes greater than about 100 individuals. GCOD's peak memory usage is lower than the other methods at most cohort sizes, with Digenic requiring the most RAM. These results establish that GCOD has intermediate computational performance.

In terms of statistical performance, GCOD performed the best. It controls the FPR very close to the targeted 5% level, with only 5.5% of pseudosibbling, 4.2% of synonymous, and 7.9% of shuffled candidate groups found to be overtransmitted (Fig. 2B). This indicates an excellent balance of power and type-I error control. Digenic also controls the FPR but is more conservative (FPR: 1.3% pseudosibbling, 2.8% synonymous, 1.3% shuffled). As a consequence, when run on nonsynonymous proband variants, GCOD identifies functionally validated gene pairs (see below), whereas Digenic does not. In contrast, RareComb is anticonservative and does not reliably control type-I error (FPR: 62% pseudosibbling, 48% synonymous, 6.5% shuffled). Because RareComb relies on control genotypes, our findings indicate that using parents as controls with this method could lead to false discoveries.

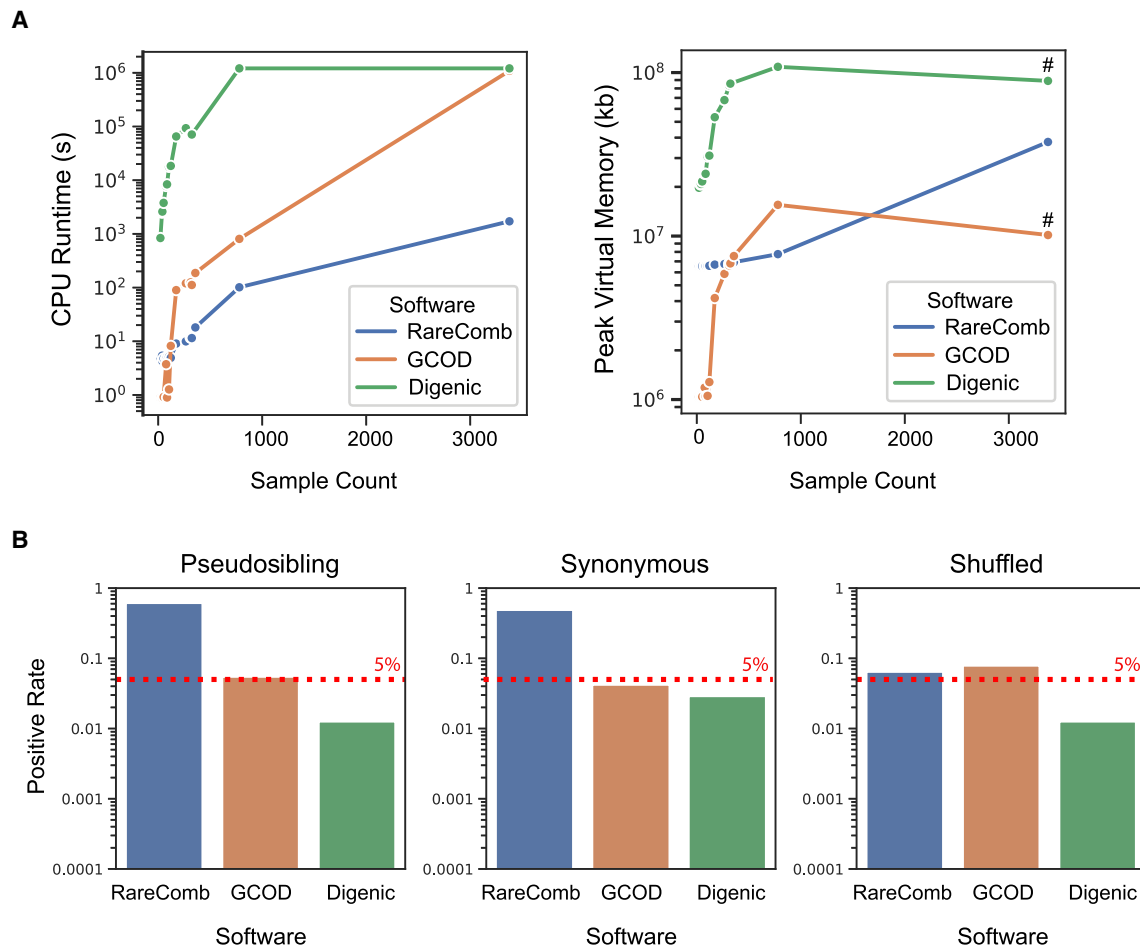


**Figure 2.** GCOD efficiently evaluates oligogenic gene sets while limiting type-I errors. (A) CPU runtime (*left*) and peak RAM usage (*right*) of GCOD and two other cohort-based oligogenic discovery software tools. Analyses were completed for the full PCGC cohort as well as smaller subdiagnoses of CHD, providing a range of sample sizes (*x*-axes). Across a range of sample sizes, GCOD's runtime is slower than RareComb's but faster than Digenic's, becoming equivalent to Digenic for the full cohort of 3377 trios (*left*). Peak memory usage is lower for GCOD compared with the other methods at most sample sizes (*right*). We note that peak memory, unlike CPU time, does not sum across multiple parallel threads; this explains the drop for peak memory in GCOD and Digenic at higher cohort sizes, which were parallelized (indicated by # for parallelized runs). (B) Type-I error rate of the three methods, using pseudosibbling variants with CADD scores in the top 0.5% exome-wide (*left*), proband synonymous variants (*center*), and variants with shuffled family IDs (*right*) as controls. GCOD controls the false-positive rate at ~5% (dashed line), whereas Digenic is relatively conservative and RareComb is anticonservative.

## CHD probands carry more oligogenic sets than familial controls

When we examined exonic variants in PCGC trios, we found that among the 227 probands with predicted-damaging de novo variants in a gene known to cause CHD in humans or mice (Richter et al. 2020), a majority (88%) inherited a predicted-damaging variant in at least one other known CHD gene (Supplemental Table S2). Given the high heritability estimates of CHD and the fact that even the relatively small number of patients with known, highly penetrant variants carry additional mutations likely to contribute to the phenotype, we hypothesized that we would find evidence of oligogenic inheritance in CHD. We applied GCOD to the rare variants ( $MAF < 0.05$ ) from PCGC trio exomes and used parental data to compute pseudosibling genotypes for each trio (Fig. 1E; Supplemental Methods; Yu and Deng 2011).

We ran GCOD at three tiers of variant severity (Supplemental Table S3), defined by nucleotide-level characteristics such as MAF and CADD score (Rentzsch et al. 2019), as well as gene-level constraint metrics like gnomAD observed-expected  $z$ -score (Karczewski et al. 2020) and  $s_{het}$  score (Cassa et al. 2017), and minimum expression level in relevant cell types (Cao et al. 2020). The strict tier includes only very rare mutations with a high probability of impairing protein function, whereas the base tier uses a more lenient cutoff scheme of the same metrics to include more candidate variants of potential interest. The CADD-based tier considers any variant predicted to be in the top 0.5% most damaging single-nucleotide variants in the genome (Rentzsch et al. 2019). Only oligogenic transmissions of a variant set were considered. To reduce false positives caused by a single driver gene with spurious cotransmitted partners, we additionally filtered oligogenic sets to those with a logistic regression interaction coefficient greater than 1.0 (Supplemental Methods).

The GCOD approach revealed 160 oligogenic gene pairs comprising 270 putative CHD risk genes at Benjamini–Hochberg  $FDR \leq 0.01$  (Supplemental Table S4). At each variant tier, we identified more oligogenic gene pairs in CHD probands compared with their pseudosiblings (Fig. 3A) and synonymous variants (Supplemental Fig. 2). These differences were all statistically significant ( $FDR$ -corrected binomial  $P \leq 0.0001$ ). At the strict tier, for example, we found 71 gene pairs overtransmitted to probands, a nearly fourfold excess compared with 19 gene pairs overtransmitted to their pseudosiblings (Table 1). Oligogenic pairs are present in a substantial number of probands, with 4% of PCGC probands carrying at least one pair at the strict tier and ~8% with more lenient tiers included.

We also computed the highest-order gene sets shared among PCGC probands at each examined tier of variant severity. Highest-order sets ranged from groups of two genes to groups of 12 genes for both probands and pseudosiblings. As with gene pairs, we find a significantly greater count of overtransmitted sets in probands compared to pseudosiblings (all Bonferroni-corrected binomial  $P < 1 \times 10^{-10}$ ) (Fig. 3B; Supplemental Table S5). In addition to the hypothesis-free approach described above, GCOD includes the option to analyze only gene combinations containing one or more user-defined candidate genes. We tested combinations of genes in the Wnt signaling pathway and the TGF-beta signaling pathway, finding seven additional oligogenic pairs composed solely of genes in these signaling pathways (Supplemental Table S6).

We next investigated whether the oligogenic pairs identified in PCGC probands include any novel CHD genes previously unidentified in smaller data sets and single-gene tests. First, we annotated which oligogenic sets contained one or more of the 744 curated human or mouse CHD genes (Richter et al. 2020).

Although more than one-third (38.8%) of proband oligogenic pairs contain at least one of these CHD genes, the vast majority of risk genes captured by GCOD were not previously known (229 of 270 genes) (Table 1). In other words, GCOD identifies sets comprising a mix of previously known and unknown genes, in which many novel potential modifier genes were overtransmitted in combination with a smaller subset of known CHD genes. We compared these findings with the results of a traditional single-gene rare variant TDT (Supplemental Methods; Supplemental Table S7). Because of a lack of significant results after multiple testing correction, we examined genes reaching significance at unadjusted  $P$ -values, nevertheless yielding threefold fewer risk genes compared with GCOD. Furthermore, GCOD's results include over fourfold more known CHD genes (41 compared to nine) (Table 1).

The genes in GCOD-identified oligogenic pairs, including the majority not previously associated with heart defects, showed significantly higher expression in the developing heart (as determined in embryonic mouse hearts at E14.5) (Zaidi et al. 2013) compared with all expressed genes, on average at the 60th percentile (Supplemental Fig. 3A). However, similar to known CHD genes, our new GCOD candidates are not restricted to being active in heart development and show broad expression across cell types and tissues. Based on data from the Protein Atlas (Uhlén et al. 2015; Karlsson et al. 2021), both known CHD genes and GCOD oligogenic genes demonstrate lower tissue specificity (Supplemental Fig. 3B) and are detected more often in many or all cell types (Supplemental Fig. 3C) compared with all gene products. Consistent with this broad activity, many GCOD known and novel candidate CHD genes are developmental transcription factors (22 in oligogenic pairs, 269 in highest order sets), which are less likely to be expressed in a tissue-specific manner compared with their targets (Sonawane et al. 2017).

In summary, GCOD identifies gene combinations transmitted more often than expected to probands, many of which include known disease genes as well as novel genes with similar patterns of expression. These findings underscore the additional signal GCOD is able to capture by collectively considering genes that tend to have rare variation together in probands, inherited separately from healthy parents.

## Genes within proband oligogenic sets are found together in canonical cardiac gene sets

To further test whether the CHD oligogenic pairs identified by GCOD comprise phenotype-relevant genes, we performed a Gene Ontology (GO) analysis. Oligogenic genes were marginally overrepresented in cellular processes related to heart development, such as atrioventricular node development (GO:0003162) and heart trabecula morphogenesis (GO:0061384;  $FDR < 0.1$ ) (Fig. 3C), as well as components generally related to cell signaling and differentiation, like receptor complex (GO:0043235) (Basson 2012) and extracellular matrix (GO:0031012) (Walma and Yamada 2020). In contrast, no GO terms were overrepresented by pseudosibling genes, supporting their utility as controls.

To provide further context for the cellular mechanisms and components implicated by GCOD, the curated set of genes previously identified as CHD-causal (Richter et al. 2020) was analyzed for enrichment of GO terms, finding a total of 1019 enriched terms at  $FDR \leq 0.05$  (Fig. 3C; Supplemental Table S8). These terms include those directly relevant to cardiogenesis and cellular differentiation, as well as terms with distinct functions but overlapping genes. We additionally noted terms that were not enriched for

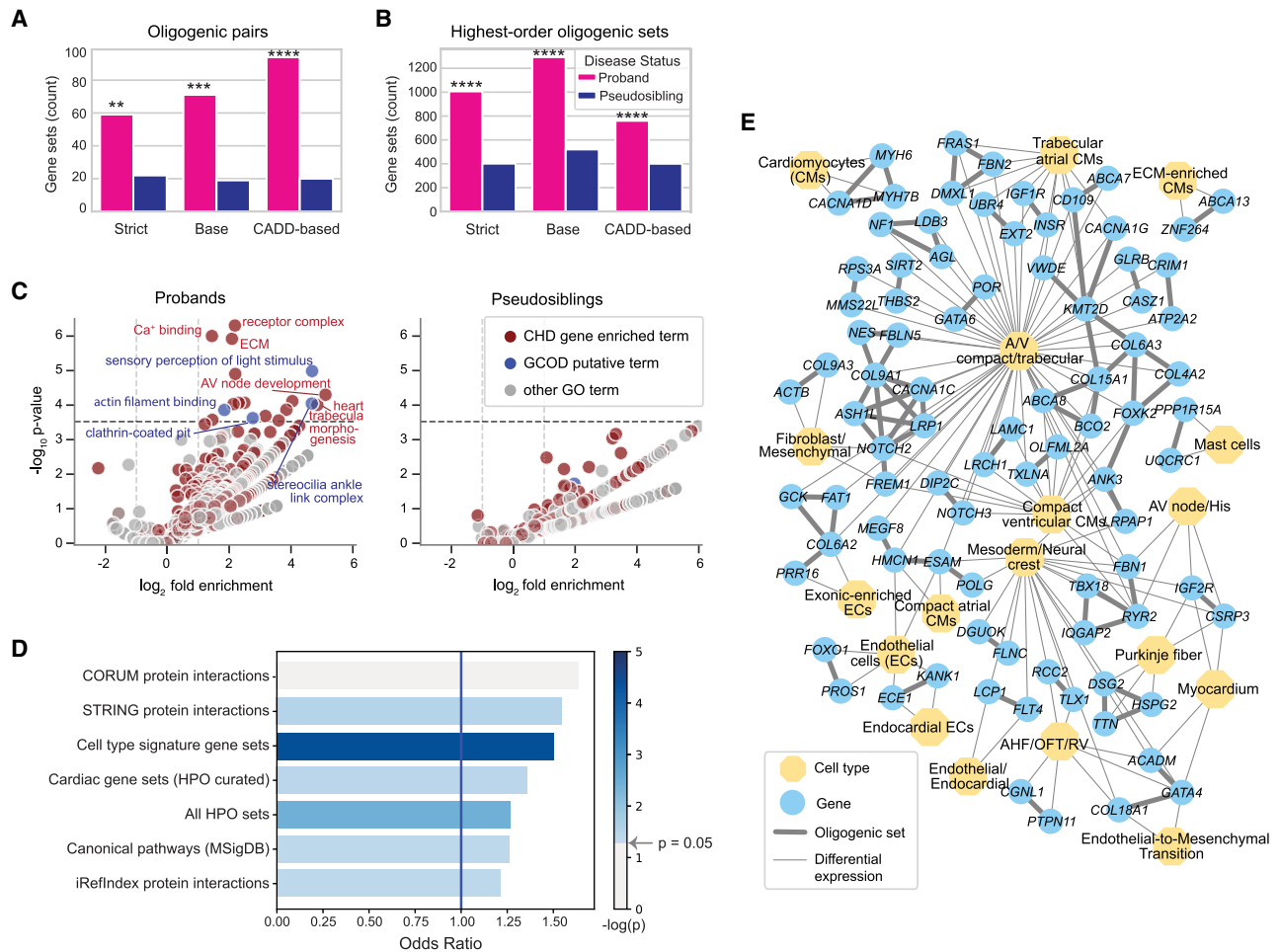


**Figure 3.** Greater number and phenotypic relevance of co-occurring gene sets in CHD probands. (A) Counts of gene pairs that were transmitted to offspring more often than expected by chance. Oligogenic pairs were found among probands at a greater rate than their pseudosibling controls for all three variant severity cutoffs, with asterisks indicating significance level: FDR-corrected  $P$ -value, (\*\*\*\*)  $P \leq 1 \times 10^{-10}$ , (\*\*\*)  $P \leq 1 \times 10^{-5}$ , (\*\*)  $P \leq 1 \times 10^{-3}$ . (B) Counts of highest-order oligogenic sets transmitted more often than expected by chance to probands and pseudosiblings. Highest-order gene sets were found among probands at a greater rate than their pseudosibling controls, with asterisks indicating significance as in A. (C) GO term enrichment of genes in CHD oligogenic pairs found in probands (left) and pseudosibling controls (right). GO terms are plotted based on fold enrichment and the inverse log of Fisher's exact test  $P$ -value. Point color indicates whether a GO term was enriched for known CHD genes or was enriched at or above marginal significance for genes in proband oligogenic pairs (indicated by the dotted line at  $FDR < 0.1$ ), but not enriched for known CHD genes. Pseudosibling set genes were not enriched for any GO terms at or above marginal significance ( $FDR = 0.1$ ). (D) Odds that at least two genes in an oligogenic set (pairs and highest-order) occurred in CHD probands and co-occur in a canonical gene set, pathway, or protein-protein interaction. Color indicates the inverse log<sub>10</sub>  $P$ -value of the odds ratio (Fisher's exact test). (HPO) Human Phenotype Ontology. (E) Network visualization of oligogenic sets containing two or more differentially expressed genes (circular nodes) identified together in at least one cardiac cell type (octagonal nodes), sourced from six studies. Thin edges indicate differential expression of a gene within the cell type compared with other study cell populations; bold edges between gene nodes indicate genes that were discovered together in a GCOD oligogenic set. (CMs) Cardiomyocytes, (ECs) endothelial cells; (A/V) atrial/ventricular, (AHF) anterior heart field, (OFT) outflow tract, (RV) right ventricle.

known CHD genes but were marginally enriched for oligogenic pair genes as discovered by GCOD (Fig. 3C). This includes actin filament binding (GO:0051015), important in cellular motility and therefore embryonic development (Pollard and Borisov 2003), and clathrin-coated pits (GO:0005905), which are a key avenue for endocytosis and were previously linked to developmental signaling (Seto et al. 2002; Robinson 2015) and heart defects (Arrigo and Lin 2021). Although few of these genes were discovered in screens of highly penetrant monogenic perturbations, our results suggest that genes related to clathrin-coated pit formation can contribute to CHD phenotypes in combination with each other or with other CHD-causing genes. The remaining novel terms, stereocilia ankle-link complex (GO:0002142) and sensory perception of light stim-

ulus (GO:0050953), contain genes associated with cell adhesion, a process with broad importance across organogenesis (Baldwin and Buck 1994).

The GO analysis above combines oligogenic sets to find common functions among all putative risk genes. We further hypothesized that genes within the same oligogenic set are more likely to be physically and/or functionally associated. To test this, we calculated the odds of an oligogenic combination being found in probands (as opposed to pseudosiblings) and co-occurring in canonical pathways, canonical gene sets, and protein-protein interactions (Fig. 3D).

GCOD-identified oligogenic sets (including pairs and highest-order gene sets) were found to comprise proteins with evidence

**Table 1.** GCOD counts of significantly overtransmitted oligogenic pairs and genes, categorized by membership to the list of 744 curated human and mouse CHD genes (Richter et al. 2020)

Tier	Disease status	No. of GCOD oligogenic pairs at FDR $\leq 0.01$	No. of unique genes in oligogenic pairs (no. of known CHD genes)	No. of (% of cohort) that carry at least one pair	No. of single TDT genes at raw $P \leq 0.01$ (no. of known CHD genes)
Strict	Proband	71	132 (23)	134 (4.0%)	31 (6)
	Pseudosibiling	19	35 (3)	42 (1.2%)	4 (0)
Base	Proband	59	109 (20)	110 (3.3%)	31 (6)
	Pseudosibiling	22	40 (3)	46 (1.4%)	3 (0)
CADD-based	Proband	94	165 (26)	163 (4.8%)	47 (5)
	Pseudosibiling	67	124 (12)	123 (3.6%)	4 (0)
Composite	Proband	160	270 (41)	266 (7.9%)	77 (9)
	Pseudosibiling	94	165 (15)	159 (4.7%)	8 (0)

Note that GCOD results use a cutoff of  $FDR \leq 0.01$ ; because no genes reached significance at that level using the rare variant TDT analysis, we report results at the level of unadjusted  $P$ -value  $\leq 0.01$  (McNemar's test).

of physical interactions more than expected, based on data from the STRING (Szklarczyk et al. 2021) and iRefIndex (Razick et al. 2008) databases (Fisher's exact test  $P$ -value  $< 0.05$  for both sets). In contrast, co-occurrences in the CORUM database of protein complexes (Steinkamp et al. 2025) were not significant; however, a relatively high odds ratio (OR) of 1.6 suggests a potential association that we are underpowered to detect owing to the smaller number of confirmed protein complexes (Fig. 3D). In total, there are 676 unique physical protein interactions in the CORUM, STRING, and iRefIndex databases (Razick et al. 2008; Szklarczyk et al. 2021; Steinkamp et al. 2025) that contain at least two genes in a GCOD set (Supplemental Table S9).

To test whether genes within an oligogenic group tend to appear together in canonical pathways, regulatory gene–target interactions, and ontology terms, we downloaded several subcollections of gene sets from the Molecular Signatures Database (MSigDB) (Subramanian et al. 2005). For each collection tested, up to several hundred gene sets are included; if at least two genes within an oligogenic set (“partners”) appear together in one or more of these canonical gene sets (e.g., a single pathway or ontology term), this is considered a co-occurrence (Fig. 3D). We found significant co-occurrence of GCOD oligogenic gene partners in cell type signature gene sets (OR=1.5, Fisher's exact test  $P=0.00004$ ), canonical pathways (OR=1.3, Fisher's exact test  $P=0.039$ ), and the Human Phenotype Ontology (HPO) as a whole (OR=1.3, Fisher's exact test  $P=0.003$ ), as well as HPO gene sets related to heart phenotypes (OR=1.4, Fisher's exact test  $P=0.036$ ). In contrast, we did not find significant enrichment for MSigDB transcription factor target sets, hallmark gene sets, or GO sets (Supplemental Fig. 4).

Significant co-occurrence within protein–protein interactions and canonical pathways indicates that the interaction (direct or indirect) of oligogenic set gene products could be relevant to disease pathogenesis. We noted a particularly strong pattern of co-occurrence among cell type signature gene sets, such that genes within CHD oligogenic groups tended to appear together as markers of particular cell clusters in single-cell expression data (Fig. 3D).

We sought to further explore this signal of cell type relevance specifically in the heart. We downloaded lists of differentially expressed genes (DEGs) of cell clusters from single-cell RNA-seq data collected during and after heart development from six sources, including adult human hearts with no cardiac

disease (Tucker et al. 2020), mice hearts collected at various time points ranging from embryonic day E7.75 to E16.5 (Li et al. 2016a; Xiao et al. 2018; de Soysa et al. 2019; Goodyer et al. 2019), and hearts from human embryos ranging from 5 to 25 weeks of gestation (Cui et al. 2019). We included a total of 140 wild-type DEG sets, defined across contexts ranging from all the major cell populations of the heart, to more specific sub-clusters like those distinguishing atrial compact cells from atrial trabecular cells. As expected, genes in CHD oligogenic sets were more likely to be differentially expressed in at least one cardiac cell type compared to the full set of human protein-coding genes (two-sample  $z$ -proportion test,  $z=2.28$ ,  $P=0.01$ ). The network of GCOD oligogenic sets in which multiple genes appeared together in a DEG set are shown in Figure 3E, with blue nodes connected by bold edges indicating genes together in a CHD oligogenic set, and thin edges connecting genes to yellow nodes of cell type clusters in which they were differentially expressed. The specific experimental context of each of the depicted cell type clusters is summarized in Supplemental Table S10.

### Diagnosis-specific risk gene interactions

Although up to this point we have analyzed oligogenic transmission frequency across the entirety of the exomes of 3377 trios in the PCGC, these probands were assessed to have myriad distinct diagnoses. To explore the possibility that similar phenotypes are caused by more similar genetic etiology, we selected several categories of CHD diagnoses to analyze separately with GCOD (Table 2). We chose six diagnoses with relatively consistent phenotypic criteria and a sample size of at least 50 probands: pulmonary atresia with intact ventricular septum (PA-IVS), truncus arteriosus (TA), tetralogy of Fallot (TOF), heterotaxy, and hypoplastic left heart syndrome (HLHS), as well as the subset of HLHS patients with both mitral atresia and aortic atresia (HLHS-MA-AA). We also curated five broader categories of CHD presentation, for example, septation defects and valvulopathies. A breakdown of which Fyler diagnoses (Béland et al. 2002) were included in each CHD category is found in Supplemental Table S11.

Several probands are included in multiple diagnostic categories. For example, a proband with a semilunar valvular defect is necessarily also included within the valvulopathy analysis, the latter category of which also includes PA-IVS. Furthermore, an individual might present with multiple distinct phenotypes like TA

**Table 2.** List of CHD subdiagnoses and categories with respective sample size of trios analyzed in this study

	Trio count
Diagnosis	
Pulmonary atresia with intact ventricular septum	52
Truncus arteriosus	76
Tetralogy of Fallot	173
Heterotaxy	266
Hypoplastic left heart syndrome (HLHS)	323
HLHS with mitral atresia and aortic atresia (HLHS-MA-AA)	104
Diagnostic category	
Atrioventricular valve	85
Semilunar valvular	121
Septation defects	312
Conotruncal (septation and spiraling)	357
Valvulopathies	780

in combination with heterotaxy. Even so, we hypothesized that analyses at varying scales of phenotypic homogeneity might better detect oligogenic sets that are specific to one or a few diagnoses but do not replicate in the entire cohort and might furthermore implicate specific genes and pathways in particular stages of heart development and the formation of specific physiological structures.

Counts of oligogenic sets in phenotypically similar subgroups corroborated our finding from the full cohort that probands harbor significantly more oligogenic sets compared to pseudosiblings (Fig. 4A). Many of these sets were found in the full PCGC data set analysis, but we find 4022 additional unique diagnosis-specific oligogenic sets among the 11 diagnoses in the strict, base, and CADD-based variant severity analyses (Supplemental Table S12). Many of these were found in the largest diagnostic categories, like valvulopathies and septation defects. However, even at the strict level, we detect the oligogenic pair *CAPN9-MGA* transmitted to just two of 52 individuals with PA-IVS (FDR=0.0004). The gene *CAPN9* has been associated previously with Noonan syndrome, which often presents with pulmonary valve stenosis and occasionally PA-IVS (Digilio and Marino 2001; Linglart and Gelb 2020). Our findings suggest the possibility of *CAPN9* involvement in the formation of the pulmonary valve along with the transcription factor *MGA* (Qin et al. 2021).

Previous research has shown a relationship between heterotaxy (left-right patterning defects that often affect the heart) and digenic combinations of variants in *DNAH6* with primary ciliary dyskinesia (PCD) genes. From sequencing data, Li et al. (2016b) found that five of six individuals with heterotaxy and carrying a *DNAH6* mutation also carried a heterozygous mutation in another PCD gene. Using a list of 51 PCD genes as curated previously (Zariwala et al. 2007; Li et al. 2016b), GCOD did not find significant overtransmission of these combinations in our broad CHD-wide analysis of the 3377 PCGC trios. However, in a diagnosis-specific analysis of 266 patients with heterotaxy, and including rare variants previously filtered by pathogenicity prediction-based cut-offs, GCOD identified several combinations of PCD genes (Supplemental Table S13): *DNAH6-DNAH11* (three probands, Benjamini–Hochberg FDR=0.006), *DNAH5-DNAH6* (two pro-

bands, Benjamini–Hochberg FDR=0.046), and *CCDC40-DNAH8* (two probands, Benjamini–Hochberg FDR=0.049). The *DNAH5-DNAH6* digenic pair was previously assayed in zebrafish, wherein the combination of two heterozygous mutations led to heterotaxy (Li et al. 2016b).

Similarly, a recent study among CHD patients with laterality defects predicted the contribution of 22 digenic pairs using a predetermined set of genes with known disease variants (Rai et al. 2025). Using more lenient variant pathogenicity criteria among specific diagnosis subgroups as above, GCOD replicated four of these gene pairs with additional modifier genes (Supplemental Table S14). For example, the predicted digenic pair *CFAP46-DNAH11* was found by GCOD in higher-order interactions among probands with septation defects, in one case a gene quad including cilia gene *CROCC2* and regulator of DNA demethylation *PROSER1* (FDR=0.01), and a quintet with cell adhesion gene *DCC*, cytoskeletal matrix gene *NEB*, and known CHD gene *RYR2* (FDR=0.004). In a broader analysis of 3910 PCGC patients, a study using case-control burden testing predicted an additional 29 digenic pairs in CHD (Kars et al. 2025). GCOD identified two of these predicted digenic pairs and found higher-order gene sets containing an additional 11 predicted digenic pairs (Supplemental Table S14).

These findings demonstrate GCOD's ability to replicate functionally validated gene combinations as well as predictions from complementary methods. It also underscores the utility of analyzing homogenous phenotypes and sets of genes larger than pairs.

#### Overlap of oligogenic sets with known protein complexes

We cross-referenced canonical protein complexes sourced from the CORUM database (Steinkamp et al. 2025) with our oligogenic sets from the combined PCGC cohort (Supplemental Tables S4, S5) and from separate diagnoses (Supplemental Table S12), finding 11 unique proband oligogenic sets in which two or more genes are known to physically interact in a protein complex. For example, the products of the *CREBBP* and *EP300* genes participate in the p300-CBP-p270-SWI/SNF complex (protein subunit symbols: EP300, CREBBP, ARID1A, SMARCA4, SMARCB1, SMARCC1, SMARCC2) and regulate histone acetyltransferase activity during development (Dallas et al. 1998; Chan and La Thangue 2001). Variants in these genes were transmitted oligogenically to two individuals in combination with the *COL6A3* gene (*COL6A3-CREBBP-EP300*, two probands with valvulopathies, FDR=0.007). Variants in these three genes were also overtransmitted independently with other genes, which led to the discovery of a network of interconnected oligogenic sets that collectively harbor multiple hits to three protein complexes: AML1-HIPK2-p300 (protein subunit symbols: RUNX1, HIPK2, EP300), RBL2 complex (protein subunit symbols: E2F4, E2F5, EP300, HDAC1, RBL2, SUV39H1), and p300-CBP-p270-SWI/SNF (Fig. 4B; Supplemental Methods).

*EP300* co-occurs with *RUNX1* in the AML1-HIPK2-p300 complex, and although the digenic pair is observed in one unaffected parent, the highest-order oligogenic set including *MYO9A* from an alternate source is only observed in CHD probands, both diagnosed with pulmonary stenosis (*EP300-MYO9A-RAD54L2-RUNX1*, two probands with valvar pulmonary stenosis, FDR=0.0002) (Fig. 4C). The protein product of *RUNX1* (previously known as AML1) forms a complex with the products of *EP300* and *CREBBP* to activate transcription and cell differentiation (Kitabayashi et al. 1998; Aikawa et al. 2006). The co-occurrence of oligogenically transmitted variants in multiple combinations of transcriptional regulators and chromatin modifiers suggests that they interact

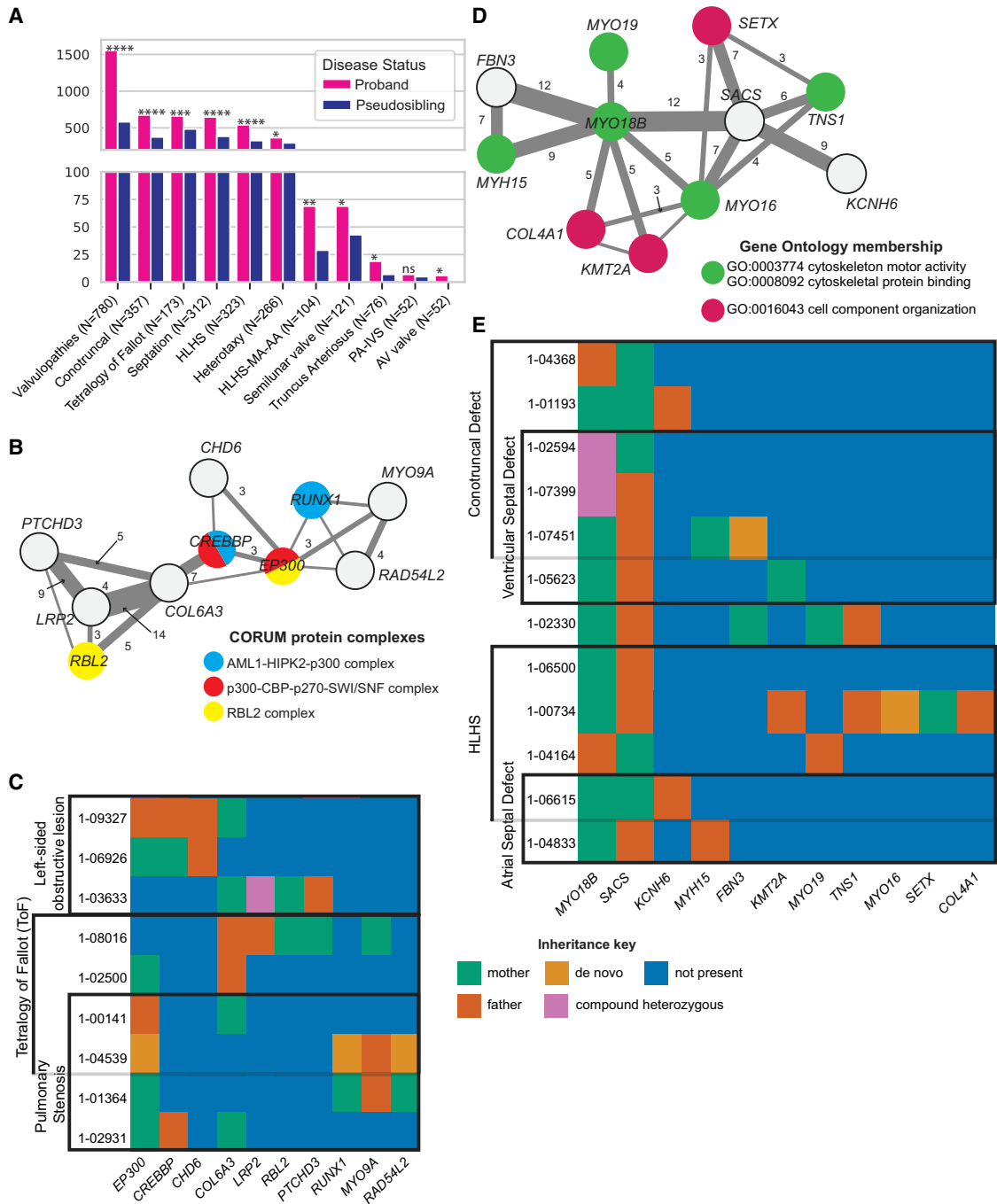


**Figure 4.** Oligogenic sets in CHDs. (A) Counts of oligogenic pairs by CHD diagnosis. (B) Network visualization of genes in oligogenic sets containing one or more of the genes coding for members of AML1-HIPK2-p300 complex, p300-CBP-p270-SWI/SNF complex, or RBL2 complex. Node color indicates a gene product's inclusion within a protein complex, and edge width and labels indicate the number of probands with co-occurring mutations in each gene pair. Nonannotated edges represent a co-occurrence count of two probands. (C) Variant inheritance matrix for genes in B. Columns indicate genes, and rows indicate probands that harbor damaging mutations in each gene. Cell color represents the parental or de novo provenance of a proband's variant(s) in the specified gene column. Multiple probands sharing a diagnosis are indicated by black boxes. (D) Network visualization of interconnected oligogenic sets, centered on the *MYO18B-SACS* digenic pair. Node color indicates a gene's association with a GO term. (E) Variant inheritance matrix for genes in D among carriers of the *MYO18B-SACS* combination.

(either directly or indirectly) in gene regulatory networks that are necessary for normal heart development. Genes not annotated with these functions, such as *COL6A3* and *MYO9A*, could be target genes or have upstream or downstream regulatory functions. For

example, the fibrillar collagen gene *COL6A3* has a role in TGF-beta signaling as previously characterized in cancers (Huang et al. 2018; Dankel et al. 2020). Given the involvement of TGF-beta signaling in epithelial-mesenchymal transformations in

cardiovascular development (Azhar et al. 2003) and its coactivation by the CBP/p300 complex (Janknecht et al. 1998), co-occurring mutations in *COL6A3*, *CREBBP*, and *EP300* could be pathogenic owing to perturbation of this pathway.

Notably, 12 probands carried predicted-damaging variants in both the *MYO18B* gene and the *SACS* gene, which encode for the myosin-18B and saccin proteins, respectively (FDR=0.002) (Fig. 4D). Ten of these observations were oligogenic transmissions in which the variants did not co-occur in an unaffected parent (Fig. 4E). The other two probands inherited *MYO18B-SACS* from their respective mothers but additionally inherited mutations in *KCNH6* from the fathers, therefore comprising an oligogenic set of three genes (Fig. 4E). Other genes found to be significantly over-transmitted with *MYO18B* and *SACS* are shown, including several involved in cytoskeletal motor activity and protein binding, as well as organization of cellular components generally (Fig. 4D). We additionally identified three oligogenic sets containing the *SACS* gene with a dynein axonemal heavy-chain gene: *DNAH2-SACS*, *DNAH7-FBN2-SACS*, and *DNAH9-SACS*. We conclude that there is an underappreciated role for the *SACS* gene in heart development, likely related to the organization and activity of structural proteins. Specifically, as *MYO18B* is known to organize thick and thin filaments in the sarcomere (Berger et al. 2017), *SACS* could play a similar or upstream/downstream role of filament organization in the heart, such that reduced function in both proteins leads to CHD. This is consistent with previous research indicating that saccin regulates filament assembly, although this was determined in neurofilaments (Gentil et al. 2019).

### Interaction of *GATA6* and *POR* in humans and mice during cardiac development

Among the hundreds of putative oligogenic gene sets prioritized by GCOD, we were particularly interested in those involving known CHD genes with prior evidence of being influenced by genetic modifiers. One such example comes from a family study in which a mutation in the known CHD gene *GATA6* was transmitted from a father to two daughters. One daughter presented with TA, whereas the father and the other daughter exhibited only milder phenotypes, such as pulmonary stenosis and atrial septal defects (ASDs) (Kodo et al. 2009). TA pathology is consistent with malfunction of normal neural crest cell migration during formation of the outflow tract (Neeb et al. 2013). When *Gata6* deletion was tested in mice in neural crest cell-specific manner, TA was only observed when both alleles of *Gata6* were deleted, which further indicates that its haploinsufficiency is an incomplete explanation for TA (Lepore et al. 2006). Moreover, *GATA6* mutations have been shown to be associated with diverse types of cardiac and pancreatic defects in human populations (Maitra et al. 2010; Allen et al. 2012; Wang et al. 2012), suggesting that mutations in additional genes could cause variable expressivity of phenotypes in patients.

We were therefore particularly interested in the *GATA6-POR* oligogenic pair identified by GCOD, which was found in three PCGC probands with TA. *POR* encodes P450 oxidoreductase, an enzyme that transfers electrons from NADPH to cytochrome P450 enzymes (Miller 2005). *Por*-null mice exhibit embryonic lethality (Shen et al. 2002; Otto et al. 2003), and severe missense mutations to *POR* (p.A287P in European ancestry and p.R457H in Japanese ancestry) cause Antley-Bixler syndrome (ABS), a skeletal malformation disorder inherited in an autosomal recessive manner (Miller et al. 2011). Notably, one study found that CHD oc-

curred in 21% of ABS cases (Oh et al. 2017), suggesting a previously underrecognized role for *POR* in heart development. Given the involvement of *POR* in retinoic acid (RA) metabolism through *CYP26* (Zlotnik et al. 2022) and given the importance of RA signaling in outflow tract and neural crest formation (Li et al. 2010; Keyte and Hutson 2012), we hypothesize that the products of *GATA6* and *POR* functionally interact during outflow tract morphogenesis and that compound damaging mutations found in these genes may have caused or contributed to TA in these patients.

The three TA patients carrying the *GATA6-POR* oligogenic pair each harbor a de novo variant in *GATA6* and an inherited predicted-damaging variant in *POR* (Fig. 5A). Interestingly, another proband in the PCGC carries a de novo *GATA6* mutation without a damaging *POR* variant and presented only with ASDs, corroborating previous findings that *GATA6* haploinsufficiency alone is not a fully penetrant cause of TA (Kodo et al. 2009). All identified variants were predicted as damaging, occur in highly conserved regions (phyloP scores > 3) near known functional domains (Fig. 5B; Supplemental Table S15), and in some cases potentially disrupt protein-DNA interaction (Supplemental Fig. 5), supporting their potential biological relevance.

To evaluate the in vivo functional consequence of the individual and combined heterozygous loss of *Gata6* and *Por*, we crossed heterozygous knockout mice of each gene. Compound heterozygous *Gata6*<sup>-/+</sup> *Por*<sup>-/+</sup> mice were born below Mendelian ratios (five observed, eight expected), although this is not a statistically significant finding (Supplemental Table S16). Notably, *Gata6*<sup>-/+</sup> *Por*<sup>-/+</sup> fetus or P0 mice exhibited ASDs or ventricular septal defects (VSDs) at a rate of 53% (nine out of 17) (Fig. 5C; Table 3), compared with littermate control WT, *Gata6*<sup>-/+</sup>, and *Por*<sup>-/+</sup> mice that experienced no clear cardiac defects by histological analyses (n=6, 11, and 9, respectively). Echocardiography performed at the adult stage demonstrated that cardiac function was affected by deficiency of *GATA6*, but not *POR*, suggesting that *POR* influences aspects of cardiac development that may be dependent on neural crest cells (Supplemental Fig. 6B).

### Discussion

Developmental phenotypes affecting the heart have profound impacts on the lives of patients and their families, and understanding the underlying cause in each case can reveal additional disease risks to monitor as the patient ages to adulthood. Evidence of oligogenic transmission of developmental disease has increased in recent years (Priest et al. 2016; Alsemari et al. 2018; Gifford et al. 2019; Mkaouar et al. 2021), necessitating a fast and accurate method to determine gene combinations of interest from patient data. We provide a computational framework called GCOD to test for the significance of oligogenic gene set transmission and report its findings from a cohort of 3377 individuals with CHD. These findings collectively contribute 229 novel potential risk genes and modifiers from 160 unique predicted-damaging gene pairs from the full cohort, as well as 2005 higher-order gene sets and 2577 gene sets found in more specific diagnostic subsets.

This software is unique compared with other recent developments in the field of oligogenic combination detection (Kerner et al. 2020; Pounraja and Girirajan 2022; Versbraegen et al. 2023) because it uses family genotypes to limit statistical inference to gene sets with oligogenic transmission and eliminates effects of population stratification, thereby reducing computation and increasing our power to detect true phenotype associations while

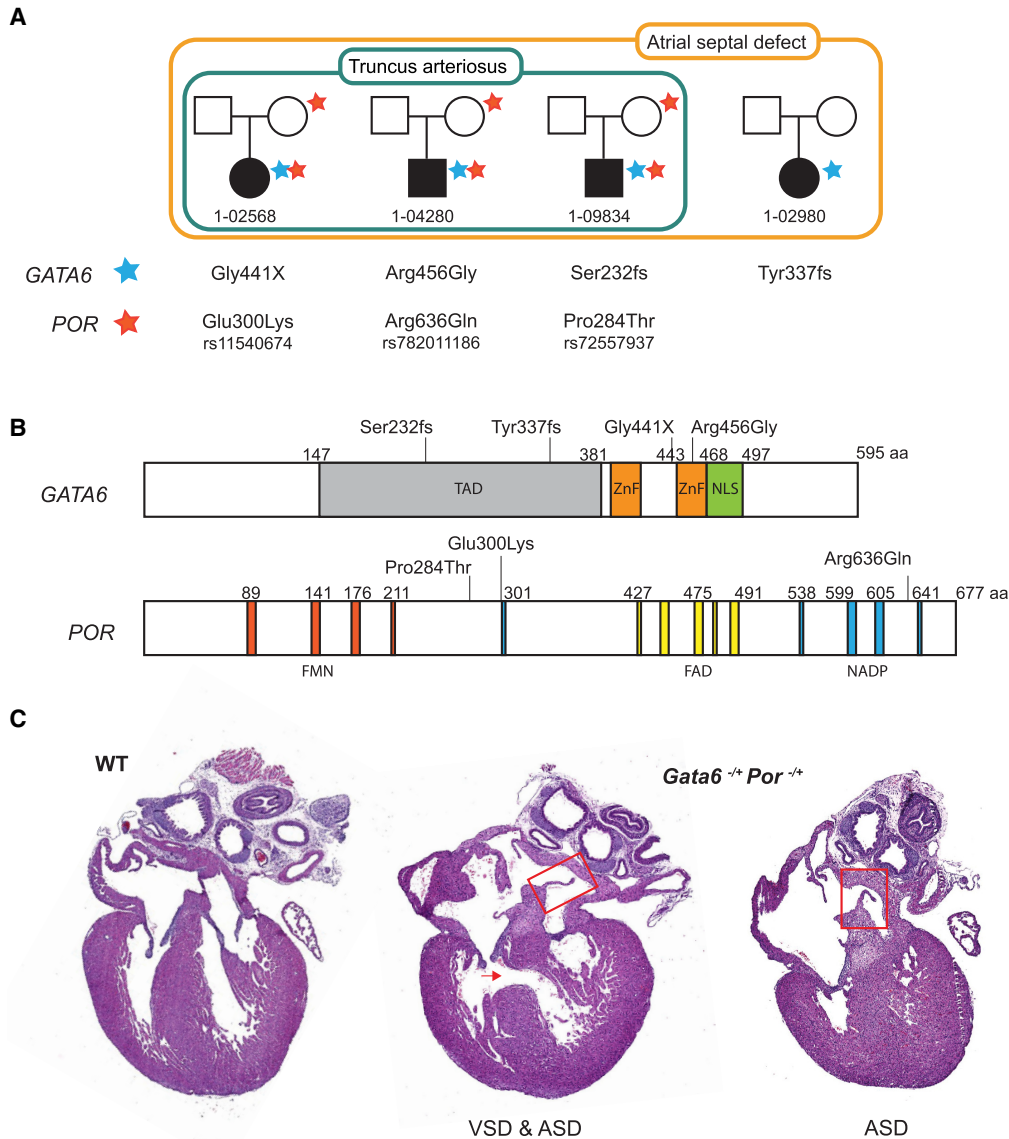


**Figure 5.** Evidence of a genetic interaction between *GATA6* and *POR* in CHD. (A) Trio pedigrees for probands with de novo *GATA6* mutation. All four probands had atrial septal defects (ASDs; larger box), whereas only three patients also had the more severe truncus arteriosus (TA) phenotype (smaller box), all of whom carry a predicted-damaging inherited mutation in *POR*. Amino acid changes to *GATA6* and *POR* are shown for each proband below. (B) Expected consequence of damaging variants in *GATA6* and *POR* protein structures. Functional domains of proteins are annotated and color-coded. (TAD) Transactivation domain, (ZnF) zinc finger domain, (NLS) nuclear localization signal, (FMN) flavin mononucleotide (FMN) binding domain, (FAD) flavin adenine dinucleotide (FAD) binding domain, (NADP) nicotinamide adenine dinucleotide phosphate (NADP) binding domain. (C) Representative histological images are shown. *Gata6*<sup>-/-</sup>; *Por*<sup>-/-</sup> compound heterozygous mice exhibit ventricular septal defects (VSDs) and/or ASDs.

controlling false positives. We have also established the concept of the “highest-order” gene set, which restricts tested candidates to only the longest set of genes unique to a group of probands and can be calculated across the cohort in a single pass rather than by specifying a gene count as in other methods (Pounraja and Girirajan 2022). We note that users should be cautious when interpreting the disease contribution of large sets of genes as they are more likely to yield false positives, owing to increasingly unlikely transmission in simulations as the number of genes increases.

Our simulation method to assess significance of oligogenic sets relies on having sequencing data from enough families to observe multiple occurrences of rare gene combinations. Even so, cli-

nicians working with one or just a few family pedigrees could make use of the first two steps of GCOD to enumerate variant and gene combinations segregating with disease to develop hypotheses for etiology in which no clear Mendelian inheritance pattern exists. The two-family filter was implemented to improve computational performance by avoiding running expensive simulations for gene pairs with insufficient statistical power. However, although our marginal *P*-values are accurate and valid for prioritizing gene sets, this prefiltering does affect the interpretation of multiple testing corrected *P*-values (FDR or Bonferroni), which are the error rates conditional on only testing pairs observed at least twice (for recommendations to obtain unconditional *P*-values, see

**Table 3.** Histological analysis of cardiac development in *Gata6* and *Por* mutant mice

	WT	<i>Gata6</i> <sup>-/+</sup>	<i>Por</i> <sup>-/+</sup>	<i>Gata6</i> <sup>-/+</sup> <i>Por</i> <sup>-/+</sup>
<b>E18.5</b>				
Samples no.	2	4	2	5
ASD only	0	0	0	1 (20%)
ASD+VSD	0	0	0	1 (20%)
Normal	2 (100%)	4 (100%)	2 (100%)	3 (60%)
<b>P0</b>				
Samples no.	4	7	7	12
ASD only	0	0	0	7 (58%)
ASD+VSD	0	0	0	0
Normal	4 (100%)	7 (100%)	7 (100%)	5 (42%)
Total (% normal)	6 (100%)	11 (100%)	9 (100%)	17 (47%)

Although 100% of wild-type, *Gata6*<sup>-/+</sup>, and *Por*<sup>-/+</sup> mice developed normal hearts, compound heterozygous *Gata6*<sup>-/+</sup> *Por*<sup>-/+</sup> mice exhibited CHDs, including atrial-septal defects (ASDs) alone or in addition to ventricular-septal defects (VSDs). At embryonic day 18.5 (E18.5), two out of five embryos displayed ASD or both ASD and VSD. At postnatal day 0 (P0), seven out of 12 pups presented with ASD.

Supplemental Methods). Developing filtering criteria that reduce computation without altering the meaning of adjusted *P*-values is an important area for future work.

GCOD is not an exhaustive search for oligogenic sets in any individual, as it does not take into account common variants (which are expected to confer less risk but undoubtedly play a role in some cases). We also do not account for the presence of noncoding variants, which can contribute to CHD and may interact with exonic variants (Richter et al. 2020; Yu et al. 2023). Including information from noncoding variants is critical to a complete understanding of the underpinnings of disease, and so, an important future direction will be to incorporate tools that predict the gene expression consequences of noncoding variants (Zhou and Troyanskaya 2015; Avsec et al. 2021; Moyon et al. 2022). Because GCOD only tests gene sets observed in at least two families, we recommend that users hoping to characterize individual cases of potentially oligogenic pathogenesis use a complementary tool such as ORVAL or Hop (Renaux et al. 2019; Gravel et al. 2024) to identify other contributing risk genes and variants in the particular case(s) of interest.

The method is more sensitive to de novo variation because an inherited event has a 50% probability of occurring, whereas most de novo events are exceedingly rare; results are therefore biased toward discovering oligogenic sets in which a nonsynonymous de novo variant was observed. In contrast, although it is useful in an individual case to particularly investigate homozygous and compound heterozygous variants that could have high impact in recessive disease, GCOD does not give additional weight to these events. Although these variants are more likely to be represented in candidate sets because they include alleles from both parents and any transmission including them is by definition oligogenic, we recommend that carrier-level post hoc investigation includes consideration of the number and zygosity of variants within genes of interest.

GCOD's estimates of variant co-occurrence will be most accurate when the tool is run with phased parental genotypes.

Incorporating phasing data is particularly useful in cases in which individual genes have multiple damaging variants in the parents. This is more likely in long genes or when using lenient cutoffs for defining damaging variants. When provided, phased genotypes can be leveraged to account for nonindependence of variants from the same haplotype. This alters GCOD's computation of the expected co-occurrence of damaging variants in a set of genes. However, GCOD analysis can proceed without phased data, as we demonstrated in our analysis of CHD in which the parental genomes were not phased.

Despite these caveats, GCOD helped expand our understanding of the genetic underpinnings of a substantial minority of CHD cases with previously cryptic causal variants (Table 1). Nearly 10% of CHD probands carry predicted-damaging variants in an oligogenic set, and many of the genes and variants GCOD prioritized are novel candidate risk factors. Experimental validation is required to determine how many of these candidate variant sets are indeed sufficient to cause a heart defect or whether some level of additional background genetic risk is necessary. These future experiments would also help to address the challenge of assessing the sensitivity and specificity of tools like GCOD, which is currently infeasible given the small number of well-characterized positive controls in the literature. A polygenic risk score approach (Wendt et al. 2020; Isgut et al. 2021) could be used to prioritize oligogenic sets that lead to disease even in otherwise relatively low-risk genomes.

Our method identified several protein complexes and functions associated with heart development and further expanded these canonical sets to include potentially interacting genes and risk modifiers. There were 568 GCOD sets for which two or more genes encode for physically interacting proteins, but we note that a solved structure for the protein interaction does not exist in most cases. It is unclear whether the variants are directly disrupting the protein interaction interface to cause disease or whether the variants separately contribute to the disruption of a related process. To determine this, future work could include a pipeline for protein folding predictions and interaction predictions using tools like AlphaFold (Evans et al. 2021; Yang et al. 2023).

The molecular mechanisms of *GATA6* and *POR* interaction during outflow tract development are not fully elucidated in this study. The PCGC proband harboring a de novo *GATA6* mutation without a *POR* variant presented only with ASD, implying that *POR* plays critical roles in aortopulmonary septation via neural crest cell migration in humans. Our mouse model clearly demonstrates that concurrent deficiency of both genes can increase severity compared with disruption of *GATA6* alone. Given that RA signaling is disrupted in *Por* knockout mice (Ribes et al. 2007; Zlotnik et al. 2022) and that *GATA6* expression can be regulated by RA signaling (Okabe and Medzhitov 2014; Zito et al. 2017), our results support a model in which *POR* modulates the phenotypic consequence of *GATA6* haploinsufficiency through the RA pathway. This interaction may contribute to the more severe cardiac defects observed in *POR*-deficient individuals and mice compared with those carrying only a single functional copy of *GATA6*.

However, we note that the penetrance of CHDs in mice is incomplete, with only half of the compound heterozygotes exhibiting defects such as muscular VSD and secundum ASDs. Furthermore, the mouse model demonstrates a different phenotypic outcome compared with what was observed in humans. *Gata6* heterozygous mice showed no morphological defects, whereas human carriers of heterozygous damaging variants in *GATA6* have ASDs. Notably, *Gata6*-*Por* compound heterozygous

mice developed ASD without TA, in contrast to human carriers of the *GATA6-POR* oligogenic combination, who were diagnosed with both ASD and TA. These interspecies differences could be owing to evolutionary divergence in cellular contributions, lineage dynamics, or the spatiotemporal regulation of the outflow tract development. The majority of *Gata6-Por* double-mutant mice exhibited secundum ASD without TA, suggesting that *Gata6-Por* compound heterozygosity was not sufficient to affect neural crest cell population in mice, resulting in normal outflow tract septation. This compensation could rise from greater functional redundancy among CYP26 genes involved in RA metabolism in mice compared with humans (Uehara et al. 2007).

Overall, we have established a framework to identify combinations of genes that are transmitted in excess to trio probands. We have provided researchers with lists of prioritized, high-confidence gene and variant combinations in CHD for high-throughput screens or more precise mechanistic experiments. GCOD is freely available for applications to other diseases and species, in hopes of moving the field toward a more complete understanding of gene interactions during development, and how genetic variants combine in disease.

## Methods

### Variant calling and filtering

WES data from the 3377 CHD trios were sequenced using the Illumina HiSeq 2000 and mapped to the GRCh37 reference genome as described previously (Zaidi et al. 2013; Jin et al. 2017; Morton et al. 2021). Uniparental disomy and structural deletions were determined using UPDio software (King et al. 2014) with default parameters. De novo variants were called using the TrioDeNovo program (Wei et al. 2015) and accepted if previously described quality conditions were met (Homsy et al. 2015). Full criteria for variant inclusion can be found in the [Supplemental Methods](#). All variants were called and are reported in GRCh37 coordinates for compatibility with Iossifov et al. (2014). These exonic variant calls would not be affected by using GRCh38, because we focus on protein-coding exons in noncentromeric regions.

### Digenic pair enumeration

GCOD creates three gene-by-family matrices, one each for the mother, father, and offspring. These three matrices store information regarding variant provenance and allele counts that is used during enumeration of gene combinations and in offspring simulations.

Let  $I$  be the number of genes and  $J$  be the number of families. The  $I$ -by- $J$  offspring matrix  $O$  contains information about damaging variants in gene  $i = 1, 2, \dots, I$  for the offspring in family  $j = 1, 2, \dots, J$ . The entries in  $O$  indicate the presence and provenance of the offspring variants using the following mutually exclusive labels:

- 0 = no variants;
- 1 = at least one variant transmitted from the mother, none transmitted from the father, no de novo variants;
- 2 = at least one variant transmitted from the father, none transmitted from the mother, no de novo variants;
- 3 = at least one variant transmitted from each parent, no de novo variants; and
- 4 = at least one de novo variant.

The  $I$ -by- $J$  maternal matrix  $M$  contains information about variants in gene  $i$  for the mother in family  $j$ . Similarly, the  $I$ -by- $J$  pa-

ternal matrix  $P$  contains information about variants in gene  $i$  for the father in family  $j$ . In both parental matrices, the entry in the  $i$ th row and  $j$ th column indicates the number of damaging alleles parent  $j$  has in gene  $i$ . For more efficient computation and storage, all three matrices are stored in compressed sparse row format.

To identify oligogenic gene pairs, the entries in  $O$  are compared for the genes in each candidate pair to determine if the damaging variant combination was present in either parent or not. For a gene pair  $(i, i')$  and family  $j$  in which neither  $O_{i,j}$  nor  $O_{i',j}$  is zero, the pair is recorded as oligogenic if there are variants in the two genes that come from different parents or if at least one of the genes has a de novo variant:

$$G_{i,i',j} = \begin{cases} 1 & \text{if } O_{i,j} \neq O_{i',j} \text{ or if } O_{i,j} > 2 \text{ or if } O_{i',j} > 2 \\ 0 & \text{otherwise} \end{cases} \quad (1)$$

In the GCOD implementation, we do not store the matrices  $G_j$  and instead only retain the identity of gene pairs  $(i, i')$  and families  $j$  in which  $G_{i,i',j} = 1$ , which avoids storing large numbers of zero entries. For gene sets larger than pairs (see section Highest-Order Gene Set Enumeration), Equation 1 is extended so that  $G_{\{i\},j} = 1$  if and only if neither parent contributed all the damaging variants in the genes in the set  $\{i\}$ ; that is, at least one variant was de novo or transmitted from the alternate parent. After identifying all combinations  $(\{i\}, j)$  with oligogenic transmission, any set  $\{i\}$  that reaches a user-specified minimum of observations in the cohort (default = 2 families:  $\sum_j G_{\{i\},j} > 2$ ) is retained as a candidate gene set for statistical testing.

### Highest-order gene set enumeration

We defined the concept of a “highest-order” gene set, which comprises the largest unique candidate set observed in two or more probands (Supplemental Fig. 1). For every pair of individuals sharing a digenic candidate, all additional damaging variant-harboring genes in common between the two individuals comprise a maximum common gene set among that pair of individuals. GCOD then checks whether any lower-order sets for a given maximum common gene set are found in additional individuals and should therefore be included as an additional highest-order candidate with a distinct transmission count. The pairwise maximum common gene sets are sorted by the number of participating genes, beginning with the largest gene set and sequentially checking against smaller gene sets common between other proband pairs. If the union of genes is greater than one, and if the variants comprising that smaller set were transmitted oligogenically in each case, then the subset becomes an additional highest-order candidate entry.

### Oligogenic transmission simulation test

For each candidate gene set  $\{i\}$ , the test statistic  $t_{\{i\}}$  is the count of the number of families in which damaging variants in the set  $\{i\}$  are inherited oligogenically:

$$t_{\{i\}} = \sum_j G_{\{i\},j} \quad (2)$$

As described above, sets with  $t_{\{i\}} < 2$  are by default not subjected to statistical testing as a means to reduce computation, although users can change this setting. Excluding sets with low counts does not alter the raw (marginal)  $P$ -values of other sets, because our simulation-based null distribution (described below) is estimated independently for each gene combination. But procedures for adjusting  $P$ -values for multiple testing are affected by the number of sets and their  $P$ -values. To include all sets for appropriate multiple testing correction, users may change the filtering threshold to zero, although this will greatly increase the computational burden of running GCOD. A more efficient option is to set the marginal

$P$ -value for all excluded sets to be equal to one (i.e., do not run the simulation) and then use all sets in the multiple testing procedure. Alternatively, one may ignore the excluded sets and then interpret the resulting adjusted  $P$ -values as conditional probabilities (i.e., the probability of the observed test statistic under the null hypothesis of random transmission *and* conditional on at least two oligogenic transmissions).

To compute  $P$ -values for the count-based test statistics  $t_{[i]}$ , we use a simulation approach. For each family, parental genotypes at loci participating in candidate sets are used to simulate  $K$  random offspring. The value  $K$  is user-defined and can be determined based on the number of candidate sets to be tested such that an alpha level of 0.05 is achievable after Bonferroni correction. The default is  $K = 10,000$  simulations with a maximum of 10,000,000 simulations to cap computational burden; this limit can be overridden, but users with large variant data sets requiring more simulations are encouraged to filter further by relevant criteria to limit compute, disk, and memory requirements. In each simulation  $k = 1, 2, \dots, K$ , for each gene  $i$  and family  $j$ , an offspring genotype is simulated by randomly selecting one allele from the father and one from the mother at each variant using the allele counts  $M_{i,j}$  and  $P_{i,j}$ . The probability of a maternally transmitted damaging variant in gene  $i$  and family  $j$  is  $1 - (0.5)^{M_{i,j}}$ , and the probability of a paternally transmitted damaging variant in gene  $i$  and family  $j$  is  $1 - (0.5)^{P_{i,j}}$ . Then, additional de novo mutations are simulated based on previously derived mutability constants (Samocha et al. 2014). If the mutability rate per chromosome for gene  $i$  is  $d_i$ , then the probability of a de novo variant in the simulated offspring is  $2 * d_i$ .

Using the resulting transmitted and de novo alleles, GCOD computes an  $I$ -by- $J$  offspring matrix  $O^k$  for simulation  $k$  using the same definitions as used above for recording the provenance of proband damaging variants, with  $O^k_{i,j}$  being equal to zero, one, two, three, or four (see section Digenic Pairs Enumeration). Repeating the simulation  $K$  times generates a distribution of  $K$  observations of  $O$  under the null hypothesis of random transmission. For each oligogenic candidate gene set  $\{i\}$ , GCOD indexes the constituent genes and uses the matrices  $\{O^1, O^2, \dots, O^K\}$  to record which simulated offspring across the  $K$  simulations carry that combination with oligogenic transmission, as described above for probands. By summing over families as in Equation 2, this generates a test statistic  $t^k_{[i]}$  for each iteration  $k$  and gene set  $\{i\}$ . For any gene set  $\{i\}$ , this provides an empirical null distribution of the number of families with oligogenic transmission (i.e.,  $K$  null values of the count statistic for that set) given the parental genotypes. The raw  $P$ -value is the proportion of iterations with a simulated test statistic as large or larger than the observed proband statistic:

$$P_{[i]} = (\sum_k t^k_{[i]} \geq t_{[i]} + 1) / (K + 1). \quad (3)$$

GCOD returns the test statistics (number of probands observed with the oligogenic combination) and  $P$ -values (raw, Benjamini-Hochberg FDR-corrected, and Bonferroni-corrected) for each candidate gene set. In this study, we use a significance threshold of Benjamini-Hochberg FDR  $\leq 0.01$  unless otherwise indicated.

### Comparison of computational resources and type-I error rate

All comparison tests were run on an Intel Xeon gold 6148 CPU @ 2.40 GHz with 40 cores (two sockets, one thread per core). CPU runtime was calculated by running all jobs with the `time` command, and summing the user and system (Sys) time spent on all parent and child processes (therefore accounting for time spent in parallel threads). Peak memory was calculated using the `memusage` package (<https://github.com/jhclark/memusage>) to report the maximum memory usage in kilobytes for the process over the course of its run, although this does not sum across parallel threads. To com-

pare the three methods' performance for the same research question, we restricted the benchmarking analysis to digenic pairs (as this is the only possible runmode for Digenic). To estimate FPR, we ran each software on all synonymous variants in the data set, on pseudosibling variants using the CADD-based variant filtering method, and on the nonsynonymous variant set in which family IDs were randomly shuffled. FPR was calculated based on the percentage of candidates that were found significant from these data; that is, if 5% of synonymous candidates were found significant by a given method, this corresponds to synonymous FPR = 0.05.

The RareComb package was run using default parameters for the `compare_enrichment()` function, using parents as controls, with a gene combination `combo_length` of two genes and `max_freq_threshold` = 0.25. To compare with GCOD, which requires at least two probands to carry an oligogenic combination, RareComb was run with `min_indv_threshold` = 2. Except when specified here, RareComb ran with default parameters.

Digenic was run in `genexgene` analysis mode. By default, digenic accepts as input two files of common and rare variants, but for our purposes, we used only rare variants (with the "common" file restricted to `Gnomad_AF1` = 0.05 and the "rare" file at `Gnomad_AF2` = 0.01). We used PLINK version 1.9 to calculate the first three principal components of genotypes in the data set, providing input for the `fen` option. Additionally, we removed the filtering step that only considers genes in which 5% of samples were carriers, instead removing pairs only observed once in the data set. Except when specified here, digenic ran with default parameters.

We also compared GCOD's performance to that of a multilocus rare-variant generalization of the TDT (mTDT). Because of the nature of our variant data set (i.e., rare variants with MAF < 0.05), we aggregated variants across the coding region of a gene using the burden of rare variants (BRV) method as done previously (Li and Leal 2008; He et al. 2014) and used a  $\chi^2$ -test with 1° of freedom to determine whether the minor alleles were transmitted together more often than expected. For a more detailed description of this method, see the Supplemental Methods.

### GO analysis and volcano plot

We performed GO analyses using the GOATOOLS package in Python3 (version 1.1.6) (Klopfenstein et al. 2018), using the `GOEnrichmentStudyNS()` function with default settings. The background gene list was genes meeting "strict" criteria and/or with DNVs in the cohort (i.e., all genes it was possible to observe in a strict oligogenic set). "CHD gene enriched terms" were found using the same analysis as described above on the set of CHD genes from Richter et al. (2020), at a cutoff of FDR < 0.05. "GCOD putative terms" were defined as any terms enriched for the list of genes in GCOD pairs (strict variant criteria) at a cutoff of FDR < 0.1 that were not also enriched for the list of known CHD genes. When reporting top enriched terms, we only include GO categories with at least five gene members for relevance and legibility.

### Canonical pathway and interaction analysis

Canonical pathways, curated signature gene sets, and ontology gene sets were sourced from MSigDB (Liberzon et al. 2015), and these were filtered to only those sets containing fewer than 500 genes. The list of cardiac gene sets curated from the HPO was created by filtering the complete HPO gene set list to those matching the name of a CHD diagnosis, as well as those containing the strings "cardiac" or "heart" (then reviewed for relevance to heart development). Protein interactions were sourced from the CORUM protein complex database (Steinkamp et al. 2025),

human physical interactions in the STRING v12.0 database (Szklarczyk et al. 2021), and human, mouse, and rat protein–protein interactions in iRefIndex v15.0 (Razick et al. 2008).

### Cell type–specific network discovery and depiction

Oligogenic sets were compared to cell type–specific DEGs sourced from previous human and mouse studies (Supplemental Table S10). Cell types containing at least two genes found in an oligogenic set together are shown in Figure 3E. We note that edges have been filtered for clarity: There are instances in which some genes depicted in Figure 3E were found together in an oligogenic set but the edge is not shown; this is the case when those oligogenic genes were not both found together in a particular cell type–specific gene set. There are likewise many instances in which genes depicted were found to be differentially expressed in more than just the cell type(s) indicated by thin edges, but we have only shown edges to cell types in which an oligogenic partner gene was also differentially expressed.

### Mouse models

*Gata6* VenusKI/+ mice (stock 028096) and *Gata6* floxed/floxed mice (stock 008196) were purchased from The Jackson Laboratory and backcrossed to C57BL/6J mice for more than five generations prior to experiments. *Por* floxed/floxed mice were generously provided by Dr. Xinxin Ding (Wu et al. 2003). Genotyping was performed according to protocols of providers. To generate whole-body knockout mice, both floxed lines were crossed with B-actin-Cre mice (Jackson Laboratory 033984), resulting in *Gata6*<sup>-/+</sup> and *Por*<sup>-/+</sup> heterozygous knockout mice, respectively. *Gata6* VenusKI/+ or *Gata6*<sup>-/+</sup> mice were crossed with *Por*<sup>-/+</sup> mice in order to examine potential cardiac phenotypes in embryos at embryonic day (E18.5) and in newborn pups at postnatal day 0 (P0). All mice were maintained under standard conditions in accordance with institutional animal care guidelines, and all procedures were conducted under protocols approved by the relevant animal ethics committee.

### Histological analysis

To examine morphological anomalies of the heart, hearts were collected and fixed in 4% paraformaldehyde in 1× PBS overnight at 4°C. The following day, samples were washed, embedded in a paraffin, and sectioned to obtain the four-chamber view of the heart. Sections were stained by hematoxylin and eosin. Each sample was evaluated by two blinded reviewers for cardiac abnormalities.

### Echocardiography

Echocardiography was performed blindly with the Vevo3100 high-resolution micro-imaging system (VisualSonics) with MX550S and MX700 ultrasound transducers. The left ventricle was assessed in both parasternal long-axis and short-axis views. To calculate the shortening fraction, left ventricular end-systolic and end-diastolic diameters were measured from the left ventricular M-mode tracing at the papillary muscle.

### Code availability

GCOD scripts are available at GitHub (<https://github.com/mepittman/gcod>) and as Supplemental Code.

### Competing interest statement

The authors declare no competing interests.

## Acknowledgments

We thank the participants and research clinicians of the Pediatric Cardiac Genomics Consortium (PCGC) and Simons Foundation Autism Research Initiative. We thank Dr. Sarah Morton of the Harvard Medical School Division of Newborn Medicine for providing data and processing pipelines from the PCGC. CHD genomic data were generated by the PCGC, under the auspices of the National Heart, Lung, and Blood Institute (NHLBI) Bench to Bassinet Program (<https://benchtoBassinet.com>). This study was funded by NHLBI (grants P01 HL098707, P01 HL146366, and UM1 HL098179), Additional Ventures, and the L.K. Whittier Foundation. M.P. was supported by an NHLBI fellowship (F31HL156439). K.L. was supported by NHLBI under award number T32HL007544-32 and F32HL158263-01. K.L. was also supported by grants from the National Research Foundation of Korea (NRF; RS-2023-00261247, RS-2023-00223069) and the Korean Fund for Regenerative Medicine (KFRM; RS-2024-00332601), funded by the Korea government (Ministry of Science and ICT).

*Author contributions:* M.P., K.L., K.S.P., and D.S. conceived and designed the study. M.P. and K.L. performed experiments. M.P. and K.L. contributed equally to this work. M.P. implemented GCOD and led the computational and statistical analyses. K.L. performed mouse experiments with the assistance of A.L. F.F. generated structural representations of GATA6 genetic variants. Y.H. performed echocardiography. M.W.C. helped K.L. with the histological analysis. M.P., K.S.P., and K.L. analyzed and interpreted data and prepared the manuscript and figures. D.S. provided critical conceptual input and oversight. K.S.P. led the study team. K.S.P., D.S., and K.L. provided funding. All authors reviewed and approved the final version.

## References

- The 1000 Genomes Project Consortium. 2015. A global reference for human genetic variation. *Nature* **526**: 68–74. doi:10.1038/nature15393
- Aikawa Y, Nguyen LA, Isono K, Takakura N, Tagata Y, Lienhard Schmitz M, Koseki H, Kitabayashi I. 2006. Roles of HIPK1 and HIPK2 in AML1- and p300-dependent transcription, hematopoiesis and blood vessel formation. *EMBO J* **25**: 3955–3965. doi:10.1038/sj.emboj.7601273
- Akhirome E, Walton NA, Noguee JM, Jay PY. 2017. The complex genetic basis of congenital heart defects. *Circ J* **81**: 629–634. doi:10.1253/circj.CJ-16-1343
- Allen HL, Flanagan SE, Shaw-Smith C, De Franco E, Akerman I, Caswell R, International Pancreatic Agenesis Consortium, Ferrer J, Hattersley AT, Ellard S. 2012. GATA6 haploinsufficiency causes pancreatic agenesis in humans. *Nat Genet* **44**: 20–22. doi:10.1038/ng.1035
- Alsemari A, Alsuhaibani M, Alhathloul R, Ali BM. 2018. Potential oligogenic disease of mental retardation, short stature, spastic paraparesis, and osteopetrosis. *Appl Clin Genet* **11**: 129–134. doi:10.2147/TACG.S172176
- Arrigo AB, Lin J-HI. 2021. Endocytic protein defects in the neural crest cell lineage and its pathway are associated with congenital heart defects. *Int J Mol Sci* **22**: 8816. doi:10.3390/ijms22168816
- Avsec Ž, Agarwal V, Visentin D, Ledsam JR, Grabska-Barwinska A, Taylor KR, Assael Y, Jumper J, Kohli P, Kelley DR. 2021. Effective gene expression prediction from sequence by integrating long-range interactions. *Nat Methods* **18**: 1196–1203. doi:10.1038/s41592-021-01252-x
- Azhar M, Schultz JEJ, Grupp I, Dorn GW II, Meneton P, Molin DGM, Gittenberger-de Groot AC, Doetschman T. 2003. Transforming growth factor beta in cardiovascular development and function. *Cytokine Growth Factor Rev* **14**: 391–407. doi:10.1016/S1359-6101(03)00044-3
- Baldwin HS, Buck CA. 1994. Integrins and other cell adhesion molecules in cardiac development. *Trends Cardiovasc Med* **4**: 178–187. doi:10.1016/1050-1738(94)90055-8
- Basson MA. 2012. Signaling in cell differentiation and morphogenesis. *Cold Spring Harb Perspect Biol* **4**: a008151. doi:10.1101/cshperspect.a008151
- Béland MJ, Jacobs JP, Tchervenkov CI, Rodney C, Franklin G, International Working Group for Mapping and Coding of Nomenclatures for Paediatric and Congenital Heart Disease. 2002. Report from the executive of the international working group for mapping and coding of nomenclatures for paediatric and congenital heart disease. *Cardiol Young* **12**: 425–430. doi:10.1017/S1047951102000732

- Berger J, Berger S, Li M, Currie PD. 2017. Myo18b is essential for sarcomere assembly in fast skeletal muscle. *Hum Mol Genet* **26**: 1146–1156. doi:10.1093/hmg/ddx025
- Cao J, O'Day DR, Pliner HA, Kingsley PD, Deng M, Daza RM, Zager MA, Aldinger KA, Blecher-Gonen R, Zhang F, et al. 2020. A human cell atlas of fetal gene expression. *Science* **370**: eaba7721. doi:10.1126/science.aba7721
- Cassa CA, Weghorn D, Balick DJ, Jordan DM, Nusinow D, Samocha KE, O'Donnell-Luria A, MacArthur DG, Daly MJ, Beier DR, et al. 2017. Estimating the selective effects of heterozygous protein-truncating variants from human exome data. *Nat Genet* **49**: 806–810. doi:10.1038/ng.3831
- Chan HM, La Thangue NB. 2001. P300/CBP proteins: HATs for transcriptional bridges and scaffolds. *J Cell Sci* **114**: 2363–2373. doi:10.1242/jcs.114.13.2363
- Cordell HJ. 2009. Detecting gene–gene interactions that underlie human diseases. *Nat Rev Genet* **10**: 392–404. doi:10.1038/nrg2579
- Cripe L, Andelfinger G, Martin LJ, Shooner K, Woodrow Benson D. 2004. Bicuspid aortic valve is heritable. *J Am Coll Cardiol* **44**: 138–143. doi:10.1016/j.jacc.2004.03.050
- Cui Y, Zheng Y, Liu X, Yan L, Fan X, Yong J, Hu Y, Dong J, Li Q, Wu X, et al. 2019. Single-cell transcriptome analysis maps the developmental track of the human heart. *Cell Rep* **26**: 1934–1950.e5. doi:10.1016/j.celrep.2019.01.079
- Dallas PB, Cheney IW, Liao D-W, Bowrin V, Byam W, Pacchione S, Kobayashi R, Yaciuk P, Moran E. 1998. P300/CREB binding protein-related protein p270 is a component of mammalian SWI/SNF complexes. *Mol Cell Biol* **18**: 3596–3603. doi:10.1128/MCB.18.6.3596
- Dankel SN, Grytten E, Bjune J-J, Nielsen HJ, Dietrich A, Blüher M, Sagen JV, Mellgren G. 2020. COL6A3 expression in adipose tissue cells is associated with levels of the homeobox transcription factor PRRX1. *Sci Rep* **10**: 20164. doi:10.1038/s41598-020-77406-2
- de Soysa TY, Ranade SS, Okawa S, Ravichandran S, Huang Y, Salunga HT, Schrickler A, Del Sol A, Gifford CA, Srivastava D. 2019. Single-cell analysis of cardiogenesis reveals basis for organ-level developmental defects. *Nature* **572**: 120–124. doi:10.1038/s41586-019-1414-x
- Digilio M, Marino B. 2001. Clinical manifestations of Noonan syndrome. *Images Paediatr Cardiol* **3**: 19–30.
- Evans R, O'Neill M, Pritzel A, Antropova N, Senior A, Green T, Židek A, Bates R, Blackwell S, Yim J, et al. 2021. Protein complex prediction with AlphaFold-multimer. bioRxiv doi:10.1101/2021.10.04.463034
- Ewens WJ. 1999. Statistical aspects of the transmission/disequilibrium test (TDT). *Lect Notes Monogr Ser* **33**: 77–94. doi:10.1214/lnms/1215455548
- Gauderman WJ. 2002. Sample size requirements for association studies of gene-gene interaction. *Am J Epidemiol* **155**: 478–484. doi:10.1093/aje/155.5.478
- Gentil BJ, Lai G-T, Menade M, Larivière R, Minotti S, Gehring K, Chapple J-P, Brais B, Durham HD. 2019. Sacsin, mutated in the ataxia ARSACS, regulates intermediate filament assembly and dynamics. *FASEB J* **33**: 2982–2994. doi:10.1096/fj.201801556R
- Gifford CA, Ranade SS, Samarakoon R, Salunga HT, de Soysa TY, Huang Y, Zhou P, Elfenbein A, Wyman SK, Bui YK, et al. 2019. Öligogenic inheritance of a human heart disease involving a genetic modifier. *Science* **364**: 865–870. doi:10.1126/science.aat5056
- Goodyer WR, Beyersdorf BM, Paik DT, Tian L, Li G, Buikema JW, Chirikian O, Choi S, Venkatraman S, Adams EL, et al. 2019. Transcriptomic profiling of the developing cardiac conduction system at single-cell resolution. *Circ Res* **125**: 379–397. doi:10.1161/CIRCRESAHA.118.314578
- Gravel B, Renaux A, Papadimitriou S, Smits G, Nowé A, Lenaerts T. 2024. Prioritization of oligogenic variant combinations in whole exomes. *Bioinformatics* **40**: btac184. doi:10.1093/bioinformatics/btac184
- He Z, O'Roak BJ, Smith JD, Wang G, Hooker S, Santos-Cortez RLP, Li B, Kan M, Krumm N, Nickerson DA, et al. 2014. Rare-variant extensions of the transmission disequilibrium test: application to autism exome sequence data. *Am J Hum Genet* **94**: 33–46. doi:10.1016/j.ajhg.2013.11.021
- He Z, Zhang D, Renton AE, Li B, Zhao L, Wang GT, Goate AM, Mayeux R, Leal SM. 2017. The rare-variant generalized disequilibrium test for association analysis of nuclear and extended pedigrees with application to Alzheimer disease WGS data. *Am J Hum Genet* **100**: 193–204. doi:10.1016/j.ajhg.2016.12.001
- Hinton RB, Martin LJ Jr, Tabangin ME, Mazwi ML, Cripe LH, Woodrow Benson D. 2007. Hypoplastic left heart syndrome is heritable. *J Am Coll Cardiol* **50**: 1590–1595. doi:10.1016/j.jacc.2007.07.021
- Hoang TT, Goldmuntz E, Roberts AE, Chung WK, Kline JK, Deanfield JE, Giardini A, Aleman A, Gelb BD, Mac Neal M, et al. 2018. The congenital heart disease genetic network study: cohort description. *PLoS One* **13**: e0191319. doi:10.1371/journal.pone.0191319
- Homsy J, Zaidi S, Shen Y, Ware JS, Samocha KE, Karczewski KJ, DePalma SR, McKean D, Wakimoto H, Gorham J, et al. 2015. De novo mutations in congenital heart disease with neurodevelopmental and other congenital anomalies. *Science* **350**: 1262–1266. doi:10.1126/science.aac9396
- Huang Y, Li G, Wang K, Mu Z, Xie Q, Qu H, Lv H, Hu B. 2018. Collagen type VI alpha 3 chain promotes epithelial-mesenchymal transition in bladder cancer cells via transforming growth factor  $\beta$  (TGF- $\beta$ )/Smad pathway. *Med Sci Monit* **24**: 5346–5354. doi:10.12659/MSM.909811
- Isgut M, Sun J, Quyyumi AA, Gibson G. 2021. Highly elevated polygenic risk scores are better predictors of myocardial infarction risk early in life than later. *Genome Med* **13**: 13. doi:10.1186/s13073-021-00828-8
- Janknecht R, Wells NJ, Hunter T. 1998. TGF-beta-stimulated cooperation of Smad proteins with the coactivators CBP/p300. *Genes Dev* **12**: 2114–2119. doi:10.1101/gad.12.14.2114
- Janku P, Robinow M, Kelly T, Bralley R, Baynes A, Edgerton MT. 1980. The van Der Woude syndrome in a large kindred: variability, penetrance, genetic risks. *Am J Med Genet* **5**: 117–123. doi:10.1002/ajmg.1320050203
- Jin SC, Homsy J, Zaidi S, Lu Q, Morton S, DePalma SR, Zeng X, Qi H, Chang W, Sierant MC, et al. 2017. Contribution of rare inherited and de novo variants in 2,871 congenital heart disease probands. *Nat Genet* **49**: 1593–1601. doi:10.1038/ng.3970
- Karczewski KJ, Francioli LC, Tiao G, Cummings BB, Alfoldi J, Wang Q, Collins RL, Laricchia KM, Ganna A, Birnbaum DP, et al. 2020. The mutational constraint spectrum quantified from variation in 141,456 humans. *Nature* **581**: 434–443. doi:10.1038/s41586-020-2308-7
- Karlsson M, Zhang C, Méar L, Zhong W, Digre A, Katona B, Sjöstedt E, Butler L, Odeberg J, Dusart P, et al. 2021. A single-cell type transcriptomics map of human tissues. *Sci Adv* **7**: eabh2169. doi:10.1126/sciadv.abh2169
- Kars ME, Stein D, Stenson PD, Cooper DN, Chung WK, Gruber PJ, Seidman CE, Shen Y, Tristani-Firouzi M, Gelb BD, et al. 2025. Deciphering the digenic architecture of congenital heart disease using trio exome sequencing data. *Am J Hum Genet* **112**: 583–598. doi:10.1016/j.ajhg.2025.01.024
- Kerner G, Bouaziz M, Cobat A, Bigio B, Timberlake AT, Bustamante J, Lifton RP, Casanova J-L, Abel L. 2020. A genome-wide case-only test for the detection of digenic inheritance in human exomes. *Proc Natl Acad Sci* **117**: 19367–19375. doi:10.1073/pnas.1920650117
- Keyte A, Hutson MR. 2012. The neural crest in cardiac congenital anomalies. *Differentiation* **84**: 25–40. doi:10.1016/j.diff.2012.04.005
- King DA, Fitzgerald TW, Miller R, Canham N, Clayton-Smith J, Johnson D, Mansour S, Stewart F, Vasudevan P, Hurles ME. 2014. A novel method for detecting uniparental disomy from trio genotypes identifies a significant excess in children with developmental disorders. *Genome Res* **24**: 673–687. doi:10.1101/gr.160465.113
- Kingdom R, Wright CF. 2022. Incomplete penetrance and variable expressivity: from clinical studies to population cohorts. *Front Genet* **13**: 920390. doi:10.3389/fgene.2022.920390
- Kitabayashi I, Yokoyama A, Shimizu K, Ohki M. 1998. Interaction and functional cooperation of the leukemia-associated factors AML1 and p300 in myeloid cell differentiation. *EMBO J* **17**: 2994–3004. doi:10.1093/emboj/17.11.2994
- Klopfenstein DV, Zhang L, Pedersen BS, Ramirez F, Vesztrocy AW, Naldi A, Mungall CJ, Yunes JM, Botvinnik O, Weigel M, et al. 2018. GOATOOLS: a Python library for gene ontology analyses. *Sci Rep* **8**: 10872. doi:10.1038/s41598-018-28948-z
- Kodo K, Nishizawa T, Furutani M, Arai S, Yamamura E, Joo K, Takahashi T, Matsuoka R, Yamagishi H. 2009. GATA6 mutations cause human cardiac outflow tract defects by disrupting semaphorin-plexin signaling. *Proc Natl Acad Sci* **106**: 13933–13938. doi:10.1073/pnas.0904744106
- Kousi M, Katsanis N. 2015. Genetic modifiers and oligogenic inheritance. *Cold Spring Harb Perspect Med* **5**: a017145. doi:10.1101/cshperspect.a017145
- Lepore JJ, Mericko PA, Cheng L, Lu MM, Morrissey EE, Parmacek MS. 2006. GATA-6 Regulates semaphorin 3C and is required in cardiac neural crest for cardiovascular morphogenesis. *J Clin Invest* **116**: 929–939. doi:10.1172/JCI27363
- Li B, Leal SM. 2008. Methods for detecting associations with rare variants for common diseases: application to analysis of sequence data. *Am J Hum Genet* **83**: 311–321. doi:10.1016/j.ajhg.2008.06.024
- Li P, Pashmforoush M, Sucov HM. 2010. Retinoic acid regulates differentiation of the secondary heart field and TGFbeta-mediated outflow tract septation. *Dev Cell* **18**: 480–485. doi:10.1016/j.devcel.2009.12.019
- Li G, Xu A, Sim S, Priest JR, Tian X, Khan T, Quertermous T, Zhou B, Tsao PS, Quake SR, et al. 2016a. Transcriptomic profiling maps anatomically patterned subpopulations among single embryonic cardiac cells. *Dev Cell* **39**: 491–507. doi:10.1016/j.devcel.2016.10.014
- Li Y, Yagi H, Onuoha EO, Damerla RR, Francis R, Furutani Y, Tariq M, King SM, Hendricks G, Cui C, et al. 2016b. DNAB6 and its interactions with PCD genes in heterotaxy and primary ciliary dyskinesia. *PLoS Genet* **12**: e1005821. doi:10.1371/journal.pgen.1005821
- Liberzon A, Birger C, Thorvaldsdóttir H, Ghandi M, Mesirov JP, Tamayo P. 2015. The Molecular Signatures Database (MSigDB) hallmark gene set collection. *Cell Syst* **1**: 417–425. doi:10.1016/j.cels.2015.12.004

- Linglart L, Gelb BD. 2020. Congenital heart defects in Noonan syndrome: diagnosis, management, and treatment. *Am J Med Genet C Semin Med Genet* **184**: 73–80. doi:10.1002/ajmg.c.31765
- Maitra M, Koenig SN, Srivastava D, Garg V. 2010. Identification of GATA6 sequence variants in patients with congenital heart defects. *Pediatr Res* **68**: 281–285. doi:10.1203/PDR.0b013e3181ed17e4
- McBride KL, Pignatelli R, Lewin M, Ho T, Fernbach S, Menesses A, Lam W, Leal SM, Kaplan N, Schliekelman P, et al. 2005. Inheritance analysis of congenital left ventricular outflow tract obstruction malformations: segregation, multiplex relative risk, and heritability. *Am J Med Genet A* **134A**: 180–186. doi:10.1002/ajmg.a.30602
- Miller WL. 2005. Minireview: regulation of steroidogenesis by electron transfer. *Endocrinology* **146**: 2544–2550. doi:10.1210/en.2005-0096
- Miller WL, Agrawal V, Sandee D, Tee MK, Huang N, Choi JH, Morrissey K, Giacomini KM. 2011. Consequences of POR mutations and polymorphisms. *Mol Cell Endocrinol* **336**: 174–179. doi:10.1016/j.mce.2010.10.022
- Mkaour R, Abdallah LCB, Naouali C, Lahbib S, Turki Z, Elouej S, Bouyacoub Y, Somai M, Mcelreavey K, Bashamboo A, et al. 2021. Oligogenic inheritance underlying incomplete penetrance of PROKR2 mutations in hypogonadotropic hypogonadism. *Front Genet* **12**: 665174. doi:10.3389/fgene.2021.665174
- Morton SU, Shimamura A, Newburger PE, Opatowsky AR, Quiat D, Pereira AC, Jin SC, Gurvitz M, Brueckner M, Chung WK, et al. 2021. Association of damaging variants in genes with increased cancer risk among patients with congenital heart disease. *JAMA Cardiol* **6**: 457–462. doi:10.1001/jamacardio.2020.4947
- Moyon L, Berthelot C, Louis A, Nguyen NTT, Crollius HR. 2022. Classification of non-coding variants with high pathogenic impact. *PLoS Genet* **18**: e1010191. doi:10.1371/journal.pgen.1010191
- Neeb Z, Lajiness JD, Bolanis E, Conway SJ. 2013. Cardiac outflow tract anomalies. *Wiley Interdiscip Rev Dev Biol* **2**: 499–530. doi:10.1002/wdev.98
- Oh J, Song JS, Park JE, Jang SY, Ki CS, Kim DK. 2017. A case of Antley-Bixler syndrome with a novel likely pathogenic variant (c.529G>C) in the *POR* gene. *Ann Lab Med* **37**: 559–562. doi:10.3343/alm.2017.37.6.559
- Okabe Y, Medzhitov R. 2014. Tissue-specific signals control reversible program of localization and functional polarization of macrophages. *Cell* **157**: 832–844. doi:10.1016/j.cell.2014.04.016
- Otto DME, Henderson CJ, Carrie D, Davey M, Gundersen TE, Blomhoff R, Adams RH, Tickle C, Wolf CR. 2003. Identification of novel roles of the cytochrome p450 system in early embryogenesis: effects on vasculogenesis and retinoic acid homeostasis. *Mol Cell Biol* **23**: 6103–6116. doi:10.1128/MCB.23.17.6103-6116.2003
- Parker LE, Landstrom AP. 2021. Genetic etiology of left-sided obstructive heart lesions: a story in development. *J Am Heart Assoc* **10**: e019006. doi:10.1161/JAHA.120.019006
- Pediatric Cardiac Genomics Consortium. 2013. The congenital heart disease genetic network study: rationale, design, and early results. *Circ Res* **112**: 698–706. doi:10.1161/CIRCRESAHA.111.300297
- Pierpont ME, Brueckner M, Chung WK, Garg V, Lacro RV, McGuire AL, Mital S, Priest JR, Pu WT, Roberts A, et al. 2018. Genetic basis for congenital heart disease: revisited: a scientific statement from the American Heart Association. *Circulation* **138**: e653–e711. doi:10.1161/CIR.0000000000000606
- Pollard TD, Borisov GG. 2003. Cellular motility driven by assembly and disassembly of actin filaments. *Cell* **112**: 453–465. doi:10.1016/S0092-8674(03)00120-X
- Pounraj VK, Girirajan S. 2022. A general framework for identifying oligogenic combinations of rare variants in complex disorders. *Genome Res* **32**: 904–915. doi:10.1101/gr.276348.121
- Priest JR, Osoegawa K, Mohammed N, Nanda V, Kundu R, Schultz K, Lammer EJ, Girirajan S, Scheetz T, Waggott D, et al. 2016. De novo and rare variants at multiple loci support the oligogenic origins of atrioventricular septal heart defects. *PLoS Genet* **12**: e1005963. doi:10.1371/journal.pgen.1005963
- Qin J, Wang C, Zhu Y, Su T, Dong L, Huang Y, Hao K. 2021. Mga safeguards embryonic stem cells from acquiring extraembryonic endoderm fates. *Sci Adv* **7**: eabe5689. doi:10.1126/sciadv.abe5689
- Rai A, Klonowski J, Yuan B, Coveler KJ, Dardas Z, Egab I, Xu J, Lupo PJ, Agopian AJ, Kostka D, et al. 2025. Genomic rare variant mechanisms for congenital cardiac laterality defect: a digenic model approach. *Am J Hum Genet* **112**: 1664–1680. doi:10.1016/j.ajhg.2025.05.014
- Razick S, Magklaras G, Donaldson IM. 2008. iRefindex: a consolidated protein interaction database with provenance. *BMC Bioinformatics* **9**: 405. doi:10.1186/1471-2105-9-405
- Renaux A, Papadimitriou S, Versbraegen N, Nachtegaal C, Boutry S, Nowé A, Smits G, Lenaerts T. 2019. ORVAL: a novel platform for the prediction and exploration of disease-causing oligogenic variant combinations. *Nucleic Acids Res* **47**: W93–W98. doi:10.1093/nar/gkz437
- Reutzsch P, Witten D, Cooper GM, Shendure J, Kircher M. 2019. CADD: predicting the deleteriousness of variants throughout the human genome. *Nucleic Acids Res* **47**: D886–D894. doi:10.1093/nar/gky1016
- Ribes V, Otto DME, Dickmann L, Schmidt K, Schuhbaur B, Henderson C, Blomhoff R, Roland Wolf C, Tickle C, Dollé P. 2007. Rescue of cytochrome P450 oxidoreductase (Por) mouse mutants reveals functions in vasculogenesis, brain and limb patterning linked to retinoic acid homeostasis. *Dev Biol* **303**: 66–81. doi:10.1016/j.ydbio.2006.10.032
- Richter F, Morton SU, Kim SW, Kitaygorodsky A, Wasson LK, Chen KM, Zhou J, Qi H, Patel N, DePalma SR, et al. 2020. Genomic analyses implicate noncoding de novo variants in congenital heart disease. *Nat Genet* **52**: 769–777. doi:10.1038/s41588-020-0652-z
- Robinson MS. 2015. Forty years of clathrin-coated vesicles. *Traffic* **16**: 1210–1238. doi:10.1111/tra.12335
- Samocha KE, Robinson EB, Sanders SJ, Stevens C, Sabo A, McGrath LM, Kosmicki JA, Rehnström K, Mallick S, Kirby A, et al. 2014. A framework for the interpretation of de novo mutation in human disease. *Nat Genet* **46**: 944–950. doi:10.1038/ng.3050
- Schaaf CP, Sabo A, Sakai Y, Crosby J, Muzny D, Hawes A, Lewis L, Akbar H, Varghese R, Boerwinkle E, et al. 2011. Oligogenic heterozygosity in individuals with high-functioning autism spectrum disorders. *Hum Mol Genet* **20**: 3366–3375. doi:10.1093/hmg/ddr243
- Schaid DJ, Sommer SS. 1994. Comparison of statistics for candidate-gene association studies using cases and parents. *Am J Hum Genet* **55**: 402–409.
- Seto ES, Bellen HJ, Lloyd TE. 2002. When cell biology meets development: endocytic regulation of signaling pathways. *Genes Dev* **16**: 1314–1336. doi:10.1101/gad.989602
- Shen AL, O'Leary KA, Kasper CB. 2002. Association of multiple developmental defects and embryonic lethality with loss of microsomal NADPH-cytochrome P450 oxidoreductase. *J Biol Chem* **277**: 6536–6541. doi:10.1074/jbc.M111408200
- Sierant MC, Jin SC, Bilguvar K, Morton SU, Dong W, Jiang W, Lu Z, Li B, López-Giráldez F, Tikhonova I, et al. 2025. Genomic analysis of 11,555 probands identifies 60 dominant congenital heart disease genes. *Proc Natl Acad Sci* **122**: e2420343122. doi:10.1073/pnas.2420343122
- Sonawane AR, Platig J, Fagny M, Chen C-Y, Paulson JN, Lopes-Ramos CM, DeMeo DL, Quackenbush J, Glass K, Kuijjer ML. 2017. Understanding tissue-specific gene regulation. *Cell Rep* **21**: 1077–1088. doi:10.1016/j.celrep.2017.10.001
- Spielman RS, McGinnis RE, Ewens WJ. 1993. Transmission test for linkage disequilibrium: the insulin gene region and insulin-dependent diabetes mellitus (IDDM). *Am J Hum Genet* **52**: 506–516.
- Steinkamp R, Tsitsiridis G, Brauner B, Montrone C, Fobo G, Frishman G, Avram S, Oprea TI, Ruepp A. 2025. CORUM in 2024: protein complexes as drug targets. *Nucleic Acids Res* **53**: D651–D657. doi:10.1093/nar/gkae1033
- Subramanian A, Tamayo P, Mootha VK, Mukherjee S, Ebert BL, Gillette MA, Paulovich A, Pomeroy SL, Golub TR, Lander ES, et al. 2005. Gene set enrichment analysis: a knowledge-based approach for interpreting genome-wide expression profiles. *Proc Natl Acad Sci* **102**: 15545–15550. doi:10.1073/pnas.0506580102
- Szklarczyk D, Gable AL, Nastou KC, Lyon D, Kirsch R, Pyysalo S, Doncheva NT, Legeay M, Fang T, Bork P, et al. 2021. The STRING database in 2021: customizable protein–protein networks, and functional characterization of user-uploaded gene/measurement sets. *Nucleic Acids Res* **49**: D605–D612. doi:10.1093/nar/gkaa1074
- Tucker NR, Chaffin M, Fleming SJ, Hall AW, Parsons VA, Bedi KC Jr, Akkad A-D, Herndon CN, Arduini A, Papangeli I, et al. 2020. Transcriptional and cellular diversity of the human heart. *Circulation* **142**: 466–482. doi:10.1161/CIRCULATIONAHA.119.045401
- Uehara M, Yashiro K, Mamiya S, Nishino J, Chambon P, Dolle P, Sakai Y. 2007. CYP26A1 and CYP26C1 cooperatively regulate anterior–posterior patterning of the developing brain and the production of migratory cranial neural crest cells in the mouse. *Dev Biol* **302**: 399–411. doi:10.1016/j.ydbio.2006.09.045
- Uhlén M, Fagerberg L, Hallström BM, Lindskog C, Oksvold P, Mardinoglu A, Sivertsson Å, Kampf C, Sjöstedt E, Asplund A, et al. 2015. Proteomics. tissue-based map of the human proteome. *Science* **347**: 1260419. doi:10.1126/science.1260419
- Veenstra-Vanderweele J, Christian SL, Cook EH Jr. 2004. Autism as a paradigmatic complex genetic disorder. *Annu Rev Genomics Hum Genet* **5**: 379–405. doi:10.1146/annurev.genom.5.061903.180050
- Versbraegen N, Gravel B, Nachtegaal C, Renaux A, Verkinderen E, Nowé A, Lenaerts T, Papadimitriou S. 2023. Faster and more accurate pathogenic combination predictions with VarCoPP2.0. *BMC Bioinformatics* **24**: 179. doi:10.1186/s12859-023-05291-3
- Walma DAC, Yamada KM. 2020. The extracellular matrix in development. *Development* **147**: dev175596. doi:10.1242/dev.175596
- Wang J, Luo X-J, Xin Y-F, Liu Y, Liu Z-M, Wang Q, Li R-G, Fang W-Y, Wang X-Z, Yang Y-Q. 2012. Novel GATA6 mutations associated with

- congenital ventricular septal defect or tetralogy of Fallot. *DNA Cell Biol* **31**: 1610–1617. doi:10.1089/dna.2012.1814
- Wei Q, Zhan X, Zhong X, Liu Y, Han Y, Chen W, Li B. 2015. A Bayesian framework for de novo mutation calling in parents-offspring trios. *Bioinformatics* **31**: 1375–1381. doi:10.1093/bioinformatics/btu839
- Wendt FR, Carvalho CM, Pathak GA, Gelernter J, Polimanti R. 2020. Polygenic risk for autism spectrum disorder associates with anger recognition in a neurodevelopment-focused phenome-wide scan of unaffected youths from a population-based cohort. *PLoS Genet* **16**: e1009036. doi:10.1371/journal.pgen.1009036
- Wenger TL, Kao C, McDonald-McGinn DM, Zackai EH, Bailey A, Schultz RT, Morrow BE, Emanuel BS, Hakonarson H. 2016. The role of mGluR copy number variation in genetic and environmental forms of syndromic autism spectrum disorder. *Sci Rep* **6**: 19372. doi:10.1038/srep19372
- Wu L, Gu J, Weng Y, Kluetzman K, Swiatek P, Behr M, Zhang Q-Y, Zhuo X, Xie Q, Ding X. 2003. Conditional knockout of the mouse NADPH-cytochrome p450 reductase gene. *Genesis* **36**: 177–181. doi:10.1002/gene.10214
- Xiao Y, Hill MC, Zhang M, Martin TJ, Morikawa Y, Wang S, Moise AR, Wythe JD, Martin JF. 2018. Hippo signaling plays an essential role in cell state transitions during cardiac fibroblast development. *Dev Cell* **45**: 153–169.e6. doi:10.1016/j.devcel.2018.03.019
- Yang Z, Zeng X, Zhao Y, Chen R. 2023. AlphaFold2 and its applications in the fields of biology and medicine. *Signal Transduct Target Ther* **8**: 115. doi:10.1038/s41392-023-01381-z
- Yu Z, Deng L. 2011. Pseudosibship methods in the case-parents design. *Stat Med* **30**: 3236–3251. doi:10.1002/sim.4397
- Yu M, Aguirre M, Jia M, Gjoni K, Cordova-Palomera A, Munger C, Amgalan D, Rosa Ma X, Pereira A, Tcheandjieu C, et al. 2023. Oligogenic architecture of rare noncoding variants distinguishes four congenital heart disease phenotypes. *Circ Genom Precis Med* **16**: 258–266. doi:10.1161/CIRCGEN.122.003968
- Zaidi S, Choi M, Wakimoto H, Ma L, Jiang J, Overton JD, Romano-Adesman A, Bjornson RD, Breitbart RE, Brown KK, et al. 2013. De novo mutations in histone-modifying genes in congenital heart disease. *Nature* **498**: 220–223. doi:10.1038/nature12141
- Zariwala MA, Knowles MR, Leigh MW. 2007. Primary ciliary dyskinesia. In *GeneReviews* (ed. Adam MP, et al.), p. 431. University of Washington, Seattle, WA.
- Zhou J, Troyanskaya OG. 2015. Predicting effects of noncoding variants with deep learning-based sequence model. *Nat Methods* **12**: 931–934. doi:10.1038/nmeth.3547
- Zito G, Naselli F, Saieva L, Raimondo S, Calabrese G, Guzzardo C, Forte S, Rolfo C, Parenti R, Alessandro R. 2017. Retinoic acid affects lung adenocarcinoma growth by inducing differentiation via GATA6 activation and EGFR and Wnt inhibition. *Sci Rep* **7**: 4770. doi:10.1038/s41598-017-05047-z
- Zlotnik D, Rabinski T, Halfon A, Anzi S, Plaschkes I, Benyamini H, Nevo Y, Gershoni OY, Rosental B, Hershkovitz E, et al. 2022. P450 oxidoreductase regulates barrier maturation by mediating retinoic acid metabolism in a model of the human BBB. *Stem Cell Reports* **17**: 2050–2063. doi:10.1016/j.stemcr.2022.07.010

Received July 1, 2025; accepted in revised form November 26, 2025.